Colloquium: Multiparticle quantum superpositions and the quantum-to-classical transition

Francesco De Martini*

Dipartimento di Fisica, Sapienza Università di Roma, I-00185 Roma, Italy and Accademia dei Lincei, via della Lungara 10, I-00165 Roma, Italy

Fabio Sciarrino†

Dipartimento di Fisica, Sapienza Università di Roma, I-00185 Roma, Italy

(published 4 December 2012)

This work reports on an extended research endeavor focused on the theoretical and experimental realization of a macroscopic quantum superposition (MQS) made up of photons. This intriguing, fundamental quantum condition is at the core of a famous argument conceived by Schrödinger in 1935. The main experimental challenge to the actual realization of this object resides generally in unavoidable and uncontrolled interactions with the environment, i.e., ''decoherence,'' leading to the cancellation of any evidence of the quantum features associated with the macroscopic system. The present scheme is based on a nonlinear process, ''quantum-injected optical parametric amplification,''which, by a linearized cloning process maps the quantum coherence of a single-particle state, i.e., a microqubit, onto a macroqubit consisting of a large number M of photons in quantum superposition. Since the adopted scheme was found resilient to decoherence, a MQS demonstration was carried out experimentally at room temperature with $M \geq 10^4$. The result led to an extended study of quantum cloning, quantum amplification, and quantum decoherence. The related theory is outlined and several experiments are reviewed, such as the test of the ''no-signaling theorem'' and the dynamical interaction of the photon MQS with a Bose-Einstein condensate. In addition, the consideration of the microqubit-macroqubit entanglement regime is extended to macroqubit-macroqubit conditions. The MQS interference patterns for large M are revealed in the experiment and bipartite microqubit-macroqubit entanglement was also demonstrated for a limited number of generated particles: $M \lesssim 12$. Finally, the perspectives opened by this new method for further studies on quantum foundations and quantum measurement are considered.

DOI: 10.1103/RevModPhys.84.1765 PACS numbers: 03.65.Ud, 03.65.Yz, 03.67.−a, 42.50.−p

CONTENTS

*francesco.demartini@uniroma1.it
†fabio.sciarrino@uniroma1.it

I. INTRODUCTION

Since the golden years of quantum mechanics (Schrödinger, 1935) the possibility of observing the quantum features of physical systems at the macroscopic level has been the object of extensive theoretical studies and recognized as a major conceptual paradigm of physics. However, in general there are severe problems preventing the observation of these features. The most important one is the unavoidable interaction with the surrounding environment, which causes the loss of any quantum coherence effect by corruption of the phase implied by any correlation of the quantum states (Zurek, 2003). Such effects are commonly believed to become increasingly severe with increase of the size of the system being studied (Raimond, Brune, and Haroche, 2001).

In the last several years many experimental attempts have been undertaken to create a superposition of multiparticle quantum states. Different experimental approaches have been pursued based on atom-photon interaction in a cavity (Raimond, Brune, and Haroche, 2001; Haroche, 2003), superconducting quantum circuits (Leggett, 2002), ions (Leibfried *et al.*, 2003, 2005; Blinov *et al.*, 2004), micromechanical sytems (Marshall *et al.*, 2003), and optical systems (Zhao *et al.*, 2004; Ourjoumtsev, 2006, 2007; Lu *et al.*, 2007). In particular, in the last few years a significant advance toward generating superposition states of large objects using optomechanical systems has been achieved (Groblacher *et al.*, 2009; Rocheleau, 2010; Teufel, 2011). When dealing with a superposition of multiparticle quantum states, there are two fundamental issues to be considered: the effective size of the superpositions and how the state behaves under decoherence (Leggett, 2002). Several criteria have been developed to establish the effective size of macroscopic superpositions in an interacting or imperfect scenario, as well as their applications to real systems (Dur, Simon, and Cirac, 2002; Leggett, 2002; Korsbakken *et al.*, 2007). A large effective size of the state usually conflicts with the robustness of the quantum superposition under interaction with the environment. Moreover, the observation of macroscopic interference phenomena requires one to conceive proper measurement strategies. In particular, one faces the problem of achieving a measurement precision that enables the observation of quantum effects at such macroscales (Kofler and Brukner, 2007).

In this paper we discuss how the amplification of quantum states can be adopted to generate multiphoton superpositions and to investigate the quantum-to-classical transition. By the present method a quantum superposition state is first generated in the microscopic (micro) world of a single-photon particle. Then, this system is mapped into the macroscopic (macro) realm by generating quantum superpositions via the well-known photon stimulation process of quantum electrodynamics (QED) in the regime of high-gain parametric amplification (De Martini, 1998a, 1998b). This approach is a natural platform for the investigation of the quantum-to-classical transition, linking quantum and classical descriptions of matter. We review the properties of the generated states in the regimes of both low and high numbers of photons. The experimental methods are outlined and the corresponding results reported and briefly described. The open question of devising a method able to experimentally demonstrate the micro-macro entanglement is finally addressed.

We first consider the regime in which a few particles are created by optical amplification of a single photon in the generic polarization state $|\phi\rangle = \alpha|H\rangle + \beta|V\rangle$, where H and V stand for horizontal and vertical polarization, respectively. This process can be related to several fundamental tasks of quantum information processing. While classical information is represented in terms of bits which can be either 0 or 1, quantum information theory is rooted in the generation and transformation of quantum bits, or qubits, which are two-dimensional quantum systems, each epitomized by a spin $\frac{1}{2}$ (Nielsen and Chuang, 2000). A qubit, unlike a classical bit, can exist in a state $|\phi\rangle$ that is a superposition of any two orthogonal basis states $\{|0\rangle, |1\rangle\}$, i.e., $|\phi\rangle = \alpha|0\rangle + \beta|1\rangle$. The fact that qubits can exist in superposition states gives unusual properties to quantum information. For instance, a fundamental issue refers to the basic limitations imposed by quantum mechanics on the set of realizable physical transformations available to the state of any quantum system. The common denominator of these bounds is that all realizable transformations have to be represented by completely positive maps, which in turn impose a constraint on the fidelity, i.e., the quantum efficiency, of the quantum measurements. For instance, the fact that an unknown qubit cannot be precisely determined (or reconstructed) by a measurement performed on a finite ensemble of identically prepared qubits implies that this state cannot be cloned, viz., copied exactly by a general transformation. In other words, the universal exact cloning map of the form $|\phi\rangle \rightarrow |\phi\rangle|\phi\rangle$, or more generally where N are cloned into $M > N$ copies, is not allowed by the rules of quantum mechanics (Wootters and Zurek, 1982). Indeed, if this were possible then one would be able to violate the bound on the fidelity of estimation, and this in turn would trigger the most dramatic changes in the present picture of the physical world. For instance, it would become possible to exploit the nonlocal quantum correlations for the superluminal exchange of meaningful information by violating the causality principle (Herbert, 1982; De Angelis *et al.*, 2007). Another map which cannot be performed exactly on an unknown qubit is the spin flip, generally dubbed universal-NOT (U-NOT) transformation. This corresponds to the operation $|\phi\rangle \rightarrow |\phi^{\perp}\rangle$, where the state $|\phi^{\perp}\rangle$ is orthogonal to the original $|\phi\rangle$ (Bechmann-Pasquinucci and Gisin, 1999; De Martini *et al.*, 2002). The quantum cloning and the NOT maps are just two among a large variety of examples realizing the effects of the essential limitations imposed by quantum mechanics on measurements and estimations.

In spite of the fact that these quantum-mechanical transformations on unknown qubits cannot be performed exactly, one may still ask what are the best possible, i.e., optimal, approximations of these maps within the given structure of quantum theory (De Martini and Sciarrino, 2005; Scarani *et al.*, 2005; Cerf and Fiurasek, 2006). In the last few years, it was found possible to associate an optimal cloning machine with a photon amplification process, e.g., by use of inverted atoms in a laser amplifier, or a nonlinear medium in a quantum-injected (QI) optical parametric amplifier (OPA) apparatus. In the case of the mode-nondegenerate QI-OPA, N photons, prepared identically in an arbitrary quantum state

$|\phi\rangle$ of polarization, are injected into the amplifier. By stimulated emission $M-N$ pairs of photons are created. In the output the amplifier generates, in the cloning mode, $M>N$ copies or clones of the input qubit $|\phi\rangle$ (De Martini *et al.*, 2002; Lamas-Linares *et al.*, 2002; De Martini, Pelliccia, and Sciarrino, 2004). Correspondingly, the amplifier generates in the output anticloning mode $M-N$ states $|\phi^{\perp}\rangle$, thus realizing a universal quantum NOT gate (De Martini *et al.*, 2002).

We now address the regime in which a large number of particles is generated by the amplification of a single photon in a quantum superposition state of polarization. Conceptually, the method consists of transferring the easily accessible condition of quantum superposition of a one-photon qubit to a mesoscopic, i.e., multiphoton, amplified state $M>1$, here referred to as a mesoscopic qubit or macroqubit. This can be done by the one-photon qubit $\alpha|H\rangle+\beta|V\rangle$ into the QI-OPA (De Martini, 1998a; De Martini, Sciarrino, and Secondi, 2005, 2009a). This process is represented in Fig. 1 which shows three possible schematic applications of the method. By virtue of the information-preserving (albeit noisy) property of the amplifier, the generated state is found to retain the same superposition character and interference properties of the injected qubit. Since the adopted scheme realizes the optimal quantum-cloning machine, able to copywith optimal fidelity any unknown input qubit , the output state will be necessarily affected by squeezed-vacuum noise arising from the input vacuum field. We now review the properties of such macrostates obtained by the quantum-injected amplification process and indicate how they can be exploited to investigate entanglement in the microscopic-macroscopic (micro-macro) regime. Precisely, an entangled photon pair is created by a nonlinear optical process; then one photon of the pair is injected into an optical parametric amplifier operating for any input polarization state (De Martini, Sciarrino, and Vitelli, 2008, 2009a). Such a transformation establishes a connection between the single-photon and the multiparticle fields. The results of a thorough theoretical analysis undertaken of this process are outlined. The results of a series of related experiments are reported. We show that, while clear experimental evidence of macroscopic quantum superposition (MQS) interference, in the absence of bipartite micro-macro entanglement, has been attained with a fairly large associated number M of particles, the micro-macro entanglement could be consistently demonstrated by an attenuation technique only for a small number of particles: $M\leq 12$. Indeed, as suggested by Sekatski *et al.* (2009) and Spagnolo *et al.* (2010) a novel *detection loophole* for large M and the need of very high measurement resolution impose severe limitations on the detection of quantum entanglement in the micro-macro regime, i.e., on the prerequisite condition for the full realization of the Schrödinger cat program. In addition, we briefly summarize the potential applications of the QI-OPA technique in different contexts, such as the realization of a nonlocality test, quantum metrology, and quantum sensing.

Finally, we consider a further approach to investigate the quantum-to-classical transition based on nonlinear parametric interactions, i.e., one that exploits the process of spontaneous parametric downconversion (SPDC) in the high-gain regime. In this framework the investigation of multiphoton states is of fundamental importance, on both the conceptual and practical levels, e.g., for nonlocality tests or for other quantum information applications. The number of photons generated depends exponentially on the nonlinear gain g of the parametric process; g can be increased by the adoption of high-power pumping lasers and high-efficiency nonlinear crystals. Different experimental approaches to generate macro-macro entangled states and to observe nonlocal correlations are reviewed (Eisenberg *et al.*, 2004; Caminati *et al.*, 2006a; De Martini, 2011; Vitelli *et al.*, 2010b). Again, the issue of high-resolution measurements arises as a fundamental ingredient for direct observation of quantum correlations in the macroscopic regime.

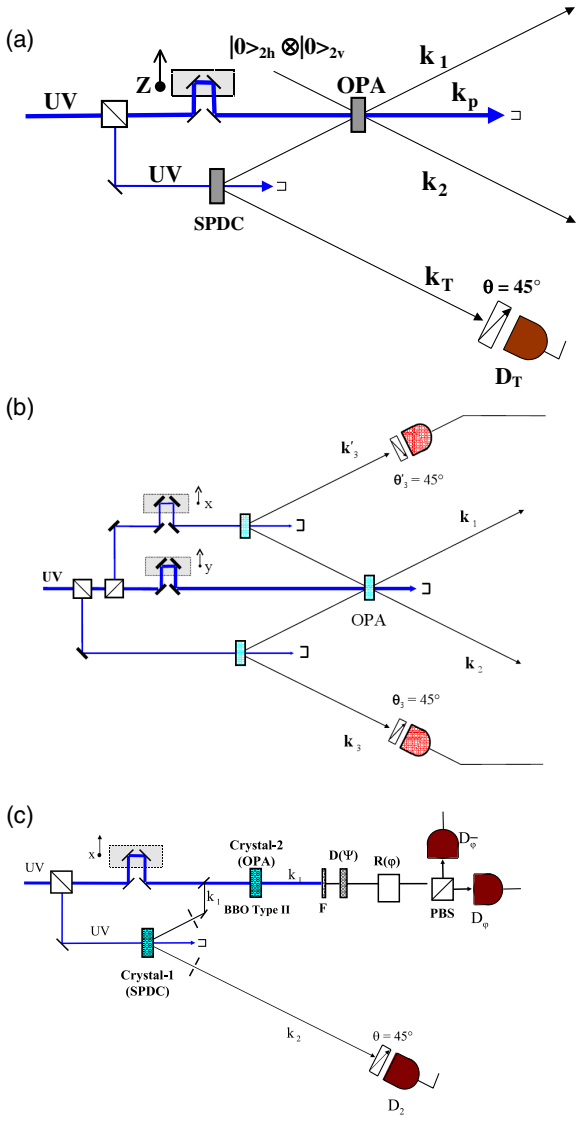

FIG. 1 (color online). Three different configurations for the amplification of quantum states. (a) Schematic diagram of a noncollinear quantum-injected optical parametric amplifier (OPA). The injection is provided by an external spontaneous parametric downconversion source of polarization-entangled photon states. From De Martini, 1998a. (b) Double injection of the optical parametric amplifier. From Bovino, De Martini, and Mussi, 1999). (c) Collinear quantum-injected optical parametric amplifier. From De Martini, 1998b.

II. OPTICAL PARAMETRIC AMPLIFICATION

We now introduce the nondegenerate optical parametric amplifier which lies at the core of the present analysis. Consider Fig. 1(a). Three different modes of the electromagnetic radiation field, say the signal $\hat{a}_1$, the idler $\hat{a}_2$, and the pump $\hat{a}_P$, are coupled by a nonlinear (NL) medium, generally a crystal, characterized by a high third-order tensor expressing the nonlinear second-order susceptibility $\chi^{(2)}$ (Yariv, 1989; Walls and Milburn, 1995; Boyd, 2008). A typical NL medium adopted in the experiments dealt with in this paper consists of a suitably cut slab of crystalline beta barium borate (BBO). Two phase-matching conditions must be satisfied during coherent three-wave interaction, viz., a scalar one, energy conservation, and a vectorial one, momentum conservation:

$$\nu_P = \nu_1 + \nu_2, \tag{1}$$

$$\vec{k}_P = \vec{k}_1 + \vec{k}_2, \tag{2}$$

where the labels $\{P, 1, 2\}$ refer to the pump, the signal, and the idler field modes, respectively. The Hamiltonian of the amplifier under the phase-matched condition (2) can be written in the rotating wave approximation as follows:

$$\hat{\mathcal{H}} = ik\hbar(\hat{a}_1^\dagger \hat{a}_2^\dagger \hat{a}_P + \hat{a}_1 \hat{a}_2 \hat{a}_P^\dagger). \tag{3}$$

The first term of the Hamiltonian (3) describes the physical process in which a photon is annihilated at frequency ν_P and twin photons are generated at frequencies ν_1 and ν_2. The second term corresponds to the inverse process. In the exact phase-matching condition the parameter k is proportional to the crystal's $\chi^{(2)}$ and to the effective crystal length l_{cryst} (Yariv, 1989; Boyd, 2008).

The Hamiltonian in Eq. (3) also describes the frequency-degenerate case, in which the frequencies associated with the modes $\hat{a}_1$ and $\hat{a}_2$ are equal but the respective wave vectors and/or polarizations are different. The quantum dynamics determined by the Hamiltonian (3) leads to a rich variety of phenomena, such as the generation of strongly correlated photon pairs by parametric downconversion (Ou and Mandel, 1988; Shih and Alley, 1988; Rarity and Tapster, 1990), quantum-injected optical parametric amplification (De Martini, 1998a), phase-insensitive amplification (Mollow and Glauber, 1967), or the generation of polarization entanglement (Kwiat *et al.*, 1995a). The unitary evolution operator associated with $\hat{\mathcal{H}}$ in the interaction picture is expressed as

$$\hat{U} = \exp[\tau(\hat{a}_1^\dagger \hat{a}_2^\dagger \hat{a}_P + \hat{a}_1 \hat{a}_2 \hat{a}_P^\dagger)], \tag{4}$$

where $\tau = kt$, and t is the interaction time.

The pump field $\hat{a}_P$ is well described by a coherent state (the quasiclassical Glauber α state), generally taken as undepleted because of the small number of converted photons compared with the very large total number of photons, typically larger than 10^{15}, associated with each pump pulse. A precise Manley-Rowe theory accounting for the pump depletion could possibly be adopted, if necessary. Hence, in the generally adopted parametric approximation the pump mode $\hat{a}_P$ is replaced by the complex amplitude of the corresponding coherent state. In that case the interaction Hamiltonian leads to the two-mode squeezing operator (Walls and Milburn, 1995)

$$\hat{S} = \exp[\tau(\alpha_P \hat{a}_1^\dagger \hat{a}_2^\dagger + \alpha_P^* \hat{a}_1 \hat{a}_2)]. \tag{5}$$

The operator $\hat{S}$ acting on the vacuum state $|0\rangle_1|0\rangle_2$ creates, via the process of SPDC a twin-beam state over the two spatial output modes $\mathbf{k}_i$ $(i = 1, 2)$ with wavelength λ_i:

$$\hat{S}|0\rangle_1|0\rangle_2 = \frac{1}{\cosh\tau} \sum_{n=0}^{\infty} \tau^n |n\rangle_1 |n\rangle_2. \tag{6}$$

The average photon numbers $\bar{n}$ in the two modes are related to the gain $g = |\tau|$ as $\bar{n} = \sinh^2 g$. We provide some numerical estimate by considering a commonly adopted apparatus. With a BBO crystal, 1 mm thick, $\lambda_P = 400$ nm, and $\lambda_1 = \lambda_2 = 800$ nm, the efficiency of the SPDC process is very low, typically around 10^{-15}.

In general, the pump field can be either a continuous or a pulsed beam (De Martini and Sciarrino, 2005). Pulsed lasers are used when a high interaction gain and/or exact knowledge of the creation time of a photon pair (a biphoton) is needed. When this is the case, mode-locked laser beams are adopted with a typical pulse duration of hundreds of femtoseconds. In SPDC two different types of phase matching (either I or II) are used, depending on the polarization of the three interacting fields, i.e., on the character of the corresponding electromagnetic waves in the birefringent nonlinear crystal, whether *ordinary* (o) or *extraordinary* (e) waves. Hereafter we consider only type-II phase matching in which the signal and idler are, respectively, o and e polarized. The spatial distribution of the emitted SPDC radiation consists of two **k**-vector cones, one for each type of wave, having common vertices coinciding with the excited spot on the NL crystal slab, which is considered very thin. We restrict our consideration for simplicity to the frequency-degenerate case only, i.e., $\nu_1 = \nu_2 = \nu_p/2$. In the case of type-II phase matching two different **k**-vector cones are emitted, the o cone and the e cone, having the same vertex and different axes, and intersecting along two straight lines. The two **k** vectors, correlated with different polarizations by the type-II parametric interaction, are parallel to these intersection lines and belong to different cones. The angle between the axes of these polarization cones can be changed by a convenient tilting of the NL slab with respect to the direction of the pump beam. When this angle is zero the two **k** vectors overlap, each one retaining its own polarization. This condition corresponds to the collinear interaction we consider shortly.

A. Noncollinear amplifier

The interaction Hamiltonian for the type-II amplifier in the noncollinear regime is given by $\hat{\mathcal{H}}_U = \imath\hbar\chi(\hat{a}_{1\psi}^\dagger \hat{a}_{2\psi_\perp}^\dagger - \hat{a}_{1\psi_\perp}^\dagger \hat{a}_{2\psi}^\dagger)$ + H.c.: see Fig. 1(a). Since this system possesses a complete SU(2) symmetry, the Hamiltonian maintains the same form for any simultaneous rotation of the Bloch sphere of the polarization basis for both output modes $\mathbf{k}_1$ and $\mathbf{k}_2$. We now analyze the features of this device when adopted in stimulated emission by a single photon with polarization $|\psi\rangle$, i.e., in the single-injection QI-OPA regime. The output state of the amplifier reads

$$|\Phi_U^{1\psi,0\psi_\perp}\rangle = \hat{U}_U|1\psi\rangle_1 = \frac{1}{C^3}\sum_{n,m=0}^{\infty}\Gamma^{n+m}(-1)^m \times\sqrt{n+1}|(n+1)\psi, m\psi_\perp\rangle_1\otimes|m\psi, n\psi_\perp\rangle_2, \tag{7}$$

where $C=\cosh g$, $\Gamma=\tanh g$, and $|p\psi, q\psi_\perp\rangle_i$ stands for a Fock state with p photons $\vec{\pi}_\psi$ polarized and q photons $\vec{\pi}_{\psi_\perp}$ polarized on spatial mode $\mathbf{k}_i$. Note that the multiparticle states $|\Phi_U^{1\psi}\rangle$, $|\Phi_U^{1\psi^\perp}\rangle$ are orthonormal.

We note that the previous expression involves superpositions of quantum states with different photon numbers. Clearly the number of photons in the pump beam will change slightly; however, the pumping beam is in a coherent state with a large number of photons. Hence this variation is negligible and the pumping beam state can be factorized.

We analyze the output field $\mathbf{k}_1$ over the polarization modes $\vec{\pi}_\pm$ when the state $|\varphi\rangle_1 = 2^{-(1/2)}(|H\rangle_1 + e^{i\varphi}|V\rangle_1)$ is injected. The average photon number $M_\pm^i$ over $\mathbf{k}_i$ with polarization $\vec{\pi}_\pm$ is found to depend on the phase φ as follows:

$$M_\pm^1(\varphi) = \bar{m} + \tfrac{1}{2}(\bar{m}+1)(1\pm\cos\varphi)\sinh^2 g, \tag{8}$$

$$M_\pm^2(\varphi) = \bar{m} + \tfrac{1}{2}\bar{m}(1\mp\cos\varphi), \tag{9}$$

with $\bar{m}=\sinh^2 g$. The conditions $\varphi=0$ and $\varphi=\pi$ correspond to single-photon injection and no injection in the mode $\vec{\pi}_\pm$, respectively. The average photon numbers related to both cases are $M_+^1(0)=2\bar{m}+1$ and $M_+^1(\pi)=\bar{m}$. The average number of photons emitted over the two polarizations over $\mathbf{k}_1$ is found to be $M=3\bar{m}+1$. The output state in mode $\mathbf{k}_1$ with polarization $\vec{\pi}_\pm$ exhibits a sinusoidal fringe pattern of the field intensity depending on φ, with a gain-dependent visibility $\mathcal{V}_U^{\rm th}=(\bar{m}+1)/(3\bar{m}+1)$ (De Martini, 1998b). Note that for $g\to\infty$, viz., $M\to\infty$, the fringe visibility attains the asymptotic values $\mathcal{V}_U^{\rm th}=\frac{1}{3}$. The former considerations are valid for any quantum state injected in the amplifier $|\phi\rangle$ when analyzed in the polarization basis $\{\vec{\pi}_\phi, \vec{\pi}_{\phi\perp}\}$.

A more sophisticated extension of the above scheme is the condition of QI-OPA double injection represented by Fig. 1(b) (Bovino, De Martini, and Mussi, 1999). Two separate SPDC sources of polarization-entangled photons are adopted to cause excitation simultaneously over the modes $\mathbf{k}_1$ and $\mathbf{k}_2$ of the QI-OPA amplifier. Meanwhile, the two photons emitted over the external modes $\mathbf{k}_3$ and $\mathbf{k}_3'$ generate, by a coincidence circuit, the overall trigger pulse for the experiment when *opposite* polarizations are realized simultaneously. Owing to the NL dynamics realized by the main NL crystal, the corresponding qubits injected in the two input QI-OPA modes $\mathbf{k}_1$ and $\mathbf{k}_2$ with different polarizations give rise to various dynamical processes within the QI-OPA amplification. For instance, they can lead to an enhanced interference-fringe visibility: $\mathcal{V}_U^{\rm th-2}=\frac{2}{3}$.

B. Collinear amplifier

We now consider the results obtained for a collinear optical configuration in which the two modes $\mathbf{k}_1$ and $\mathbf{k}_2$ are made to overlap: see Fig. 1(c). The interaction Hamiltonian of this process is $\hat{\mathcal{H}}_{\rm PC}=\imath\hbar\chi\hat{a}_H^\dagger\hat{a}_V^\dagger+\text{H.c.}$ in the $\{\vec{\pi}_H, \vec{\pi}_V\}$ polarization basis. The same Hamiltonian is expressed as $\hat{\mathcal{H}}_{\rm PC}=(i\hbar\chi/2)e^{-i\phi}(\hat{a}_\phi^{\dagger 2}-\hat{a}_{\phi\perp}^{\dagger 2})+\text{H.c.}$ for any equatorial basis $\{\vec{\pi}_\phi, \vec{\pi}_{\phi\perp}\}$ on the Poincaré sphere having as poles the states $\vec{\pi}_H$ and $\vec{\pi}_V$. The amplified state for an injected equatorial qubit $|\varphi\rangle_1$ is

$$|\Phi_{\rm PC}^\phi\rangle = \hat{U}_{\rm PC}|1\varphi, 0\varphi_\perp\rangle_1 = \sum_{i,j=0}^{\infty}\gamma_{ij}|(2i+1)\varphi, (2j)\varphi_\perp\rangle_1, \tag{10}$$

where

$$\gamma_{ij}=\frac{1}{C^2}\left(e^{-\imath\varphi}\frac{\Gamma}{2}\right)^i\left(-e^{-\imath\varphi}\frac{\Gamma}{2}\right)^j\frac{\sqrt{(2i+1)!}\sqrt{(2j)!}}{i!j!},$$

$C=\cosh g$, and $\Gamma=\tanh g$.

The average photon number $M_\pm$ over $\mathbf{k}_1$ with polarization $\vec{\pi}_\pm$ is found to depend on the phase φ as $M_\pm(\varphi)=\bar{m}+\frac{1}{2}\times(2\bar{m}+1)(1\pm\cos\varphi)$ with $\bar{m}=\sinh^2 g$. The average photon number related to both cases is $M_+(0)=3\bar{m}+1$ and $M_+(\pi)=\bar{m}$. The average number of photons emitted over the two polarizations over $\mathbf{k}_1$ is found to be $M=4\bar{m}+1$. The sinusoidal fringe pattern of the field intensity has visibility of $\mathcal{V}_{\rm PC}^{\rm th}=(2\bar{m}+1)/(4\bar{m}+1)$ (De Martini, 1998b). Note that for $g\to\infty$, the fringe visibility attains the asymptotic value $\mathcal{V}_{\rm PC}^{\rm th}=\frac{1}{2}$.

III. OPTIMAL QUANTUM MACHINES VIA PARAMETRIC AMPLIFICATION

In the early 1980s Ghirardi (1981), Dieks (1982), and Wootters and Zurek (1982) demonstrated the impossibility of perfectly copying an unknown arbitrary quantum state. In other words, a universal machine mapping $|\Psi\rangle\to|\Psi\rangle|\Psi\rangle$ for every $|\Psi\rangle$ cannot be physically realized. More generally, an exact, universal cloner of N qubits into $M>N$ qubits cannot exist. Of course perfect cloning can be provided by a nonuniversal cloning machine, i.e., one made for one or a restricted class of states. Consider the following scenario: In order to copy the quantum state of qubit C, we couple it with another ancilla T in the state $|0\rangle$ by adopting a two-qubit logical gate: a control-NOT (C-NOT) gate. By this approach it is possible to perfectly copy the state $|0\rangle_C$ or $|1\rangle_C$ using the qubit to be copied as a control qubit and an ancilla qubit in the state $|0\rangle_T$ as the target (Nielsen and Chuang, 2000). However, starting from any general state $|\phi\rangle_C=\alpha|0\rangle_C+\beta|1\rangle_C$, the output state generated by the C-NOT gate is $\alpha|0\rangle_C|0\rangle_T+\beta|1\rangle_C|1\rangle_T$ with $\rho_C=\rho_T=|\alpha|^2|0\rangle\langle 0|+|\beta|^2|1\rangle\langle 1|$, which is clearly different from the initial state $|\phi\rangle\langle\phi|$. Hence the quantum C-NOT gate realizes a perfect cloning machine only for the two input qubits belonging to the set $\{|0\rangle, |1\rangle\}$. Of course these limitations are effective within the quantum world, i.e., whenever the quantum superposition character of the state dynamics is a necessary property of the system, as in an interferometer or, more generally, in a quantum computer.

The no-cloning theorem has also interesting connections with the impossibility of superluminal communication (generally called the no-signaling condition) (Simon, Bužek, and Gisin, 2001). That condition will be discussed in detail in Sec. IV.

We shall see that an approximate optimal solution for cloning as well as for other quantum processes which are impossible in their exact form is possible. By definition, the optimal solutions correspond to the best maps realizable by nature, i.e., the ones that work just on the boundaries corresponding to the limitations imposed by the principles of quantum mechanics.

The concept of an optimal cloning process was first worked out by Buzek and Hillery (1996). A transformation which produces two copies ($M = 2$) in the same mixed state ρ_{Cl} out of an arbitrary input qubit $|\phi\rangle$ ($N = 1$) was introduced with a fidelity equal to

$$\mathcal{F}_{1\to 2}(|\phi\rangle, \rho_{\mathrm{Cl}}) = \langle\phi|\rho_{\mathrm{Cl}}|\phi\rangle = \tfrac{5}{6}. \tag{11}$$

This map was demonstrated to be optimal in the sense that it maximizes the average fidelity between the input state and output qubits by Gisin and Massar (1997), Bruß *et al.* (1998), Bruss, Ekert, and Macchiavello (1998), and Werner (1998). More generally, Gisin and Massar (1997) investigated quantum-cloning machine which transforms N identical qubits into M identical copies with an optimal fidelity. In summary, the universal quantum-cloning machine, which transforms N identical qubits $|\phi\rangle$ into M identical copies ρ_{Cl}, achieves as optimal fidelity

$$\mathcal{F}_{N\to M}(|\phi\rangle, \rho_{\mathrm{Cl}}) = \frac{N + 1 + \beta}{N + 2}, \tag{12}$$

with $\beta \equiv N/M \leq 1$ (Gisin and Massar, 1997; Bruss, Ekert, and Macchiavello, 1998; Buzek and Hillery, 1998). It is useful to compare the previous approach with the process of state estimation. Suppose that we have N copies of the same quantum state $|\varphi\rangle$ and we wish to determine all the parameters which characterize $|\varphi\rangle$. The optimal estimation procedure leads to a fidelity between the input and the estimated states equal to $\mathcal{F}_{\mathrm{est}} = (N + 1)/(N + 2)$. As we can see, $\mathcal{F}_{N\to M}(|\phi\rangle, \rho_{\mathrm{Cl}})$ is larger than the fidelity obtained by the N estimation approach and reduces to the result for $\beta \to 0$, i.e., for an infinite number of copies $M \to \infty$. The extra positive term β in the above expression accounts for the excess of quantum information which, originally stored in N states, is optimally redistributed by entanglement among the $M - N$ remaining blank ancilla qubits (Buzek and Hillery, 1996).

In addition to the above results, less universal cloning machines have been investigated (Buzek *et al.*, 1997; Bruss, Ekert, and Macchiavello, 1998), where the state-dependent cloner is optimal with respect to a given ensemble of states. As discussed later, this process, generally referred to as covariant cloning, operates with a higher fidelity than for the universal cloning since there is a partial *a priori* knowledge of the state (11).

The study of optimal quantum cloning is interesting since it implies an insightful understanding of the critical boundaries existing between classical and quantum information processing. In the quantum information perspective, the optimal cloning process may be viewed as providing a distribution of quantum information over a larger system in the most efficient way (Ricci *et al.*, 2005). More details on the general cloning process can be found in De Martini and Sciarrino (2005), Scarani *et al.* (2005), and Cerf and Fiurasek (2006).

A. Universal optimal quantum cloning

Since the first articles on the no-cloning theorem were published, it has been proposed that the QED stimulated emission process be exploited in order to make imperfect copies of the polarization state of single photons (Milonni and Hardies, 1982; Mandel, 1983). De Martini (1998a), De Martini, Mussi, and Bovino (2000), and Simon, Weihs, and Zeilinger (2000) showed that the optimal universal quantum cloning can indeed be realized by this method. If polarization encoding is adopted, the universality of this scheme is achieved by choosing systems that have appropriate symmetries, i.e., having a stimulated emission gain g which is polarization independent. This condition can be achieved by adopting a laser medium or a QI-OPA amplifier working in the noncollinear configuration. This section deals explicitly with this scheme.

For the first scenario we consider $1 \to 2$ universal cloning. Precisely the action of the cloner can be described by the following covariant transformation (Buzek and Hillery, 1996):

$$|\Psi\rangle_{C1}|0\rangle_{C2}|0\rangle_{\mathrm{AC}} \Rightarrow \sqrt{2/3}|\Psi\rangle_{C1}|\Psi\rangle_{C2}|\Psi^{\perp}\rangle_{\mathrm{AC}} - \sqrt{1/3}|\{\Psi, \Psi^{\perp}\}\rangle_{C1,C2}|\Psi\rangle_{\mathrm{AC}}, \tag{13}$$

where the first state vector, on the left-hand side of Eq. (13), corresponds to the system to be cloned, the second state vector describes the system on which the information is to be copied (blank qubit), represented by the *cloning channel* (C), the mode $\mathbf{k}_1$, while the third state vector represents the cloner machine. The blank qubit and the cloner are initially in the known state $|0\rangle$. The state $|\{\Psi, \Psi^{\perp}\}\rangle$ is the symmetrized state of the two qubits: $2^{-1/2}(|\Psi\rangle|\Psi^{\perp}\rangle + |\Psi^{\perp}\rangle|\Psi\rangle)$.

At the outputs of the cloners $C1$ and $C2$, we find two qubits, the original and the copy, each one with the following density matrix:

$$\rho_{C1} = \rho_{C2} = \tfrac{5}{6}|\Psi\rangle\langle\Psi| + \tfrac{1}{6}|\Psi^{\perp}\rangle\langle\Psi^{\perp}|. \tag{14}$$

The density operators ρ_{C1} and ρ_{C2} describe the best possible approximation of the perfect universal cloning process. The fidelity of this transformation does not depend on the state of the input and is equal to Eq. (12). The cloner itself after the cloning transformation is in the state $\rho_{\mathrm{AC}} = \frac{1}{3}|\Psi^{\perp}\rangle\langle\Psi^{\perp}| + \frac{1}{3} \times \mathbf{I}$, where $\mathbf{I}$ is the unity operator and is related to the universal-NOT gate, as we see later (see Fig. 2).

We now establish a close connection of the above cloning results with the noncollinear QI-OPA system. The photon injected in the mode $\mathbf{k}_1$ has a generic polarization state corresponding to the unknown input qubit $|\Psi\rangle$. We describe this polarization state as $\hat{a}^{\dagger}_{\Psi}|0, 0\rangle_1 = |1, 0\rangle_1$, where $|m, n\rangle_1$ represents a state with m photons having the polarization Ψ, and n photons with polarization $\Psi^{\perp}$ on the mode $\mathbf{k}_1$. We assume that the mode $\mathbf{k}_2$ is initially in the vacuum state. The initial polarization state is hence expressed as $|\Psi\rangle_{\mathrm{in}} = |1, 0\rangle_1 \otimes |0, 0\rangle_2$ and evolves according to the unitary operator $\hat{U}_U \equiv \exp(-i\hat{H}_U t/\hbar)$ (see Sec. II.A):

$$\hat{U}_U|\Psi\rangle_{\mathrm{in}} \simeq |1, 0\rangle_1 \otimes |0, 0\rangle_2 + g(\sqrt{2}|2, 0\rangle_1 \otimes |0, 1\rangle_2 - |1, 1\rangle_1 \otimes |1, 0\rangle_2). \tag{15}$$

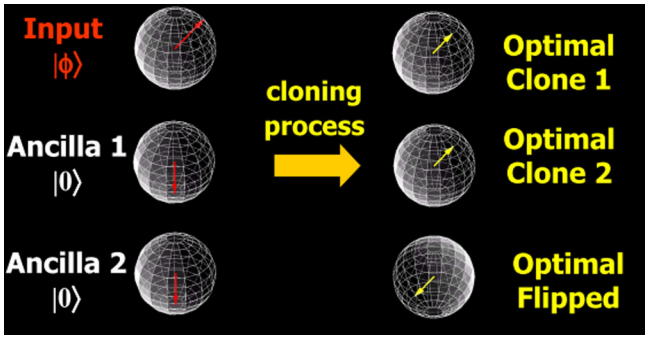

FIG. 2 (color online). Scheme of the optimal cloning process. The input and output qubits are represented on the Bloch sphere. The vectors associated with the output states are shrunk compared to the input state $|\phi\rangle$.

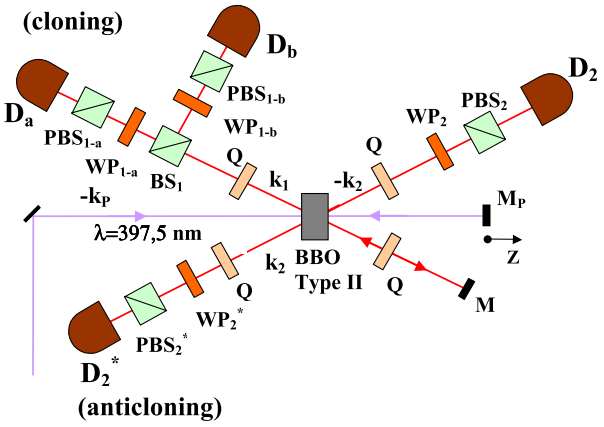

FIG. 3 (color online). Schematic diagram of the universal optimal cloning machine realized on the cloning (C) channel (mode $\mathbf{k}_1$) of a *self-injected* OPA and of the universal-NOT gate realized on the anticloning (AC) channel, $\mathbf{k}_2$. From De Martini, Pelliccia, and Sciarrino, 2004.

The linearization procedure implying the above approximation is justified in the present scenario by the small value of the amplification gain $g \approx 0.1$ (De Martini *et al.*, 2002; De Martini, Pelliccia, and Sciarrino, 2004). The zero-order term in Eq. (15) corresponds to the process when the input photon in the mode $\mathbf{k}_1$ did not interact in the nonlinear medium, while the second term describes the first-order amplification process. Here the state $|2, 0\rangle_1$ describing two photons of the mode $\mathbf{k}_1$ in the polarization state Ψ corresponds to the state $|\Psi\Psi\rangle$.

To see that the stimulated emission is indeed responsible for creation of the cloned qubit, we compare the state Eq. (15) with the output of the optical parametric amplifier when the vacuum is injected into the crystal in both input modes $\mathbf{k}_i$ ($i = 1, 2$). In this SPDC case the input state is $|0\rangle_{\text{in}} = |0, 0\rangle_1 \otimes |0, 0\rangle_2$, and we obtain to the same order of approximation as above

$$\hat{U}_U|0\rangle_{\text{in}} \simeq |0, 0\rangle_1 \otimes |0, 0\rangle_2 + g(|1, 0\rangle_1 \otimes |0, 1\rangle_2 - |0, 1\rangle_1 \otimes |1, 0\rangle_2). \tag{16}$$

We see that the cloned qubits described by the state vector $|1, 0\rangle_1$ on the right-hand sides of Eqs. (15) and (16), appear with different amplitudes, corresponding to the ratio of the probabilities $R = 2$. It is easy to show that the fidelity of the output clone is $(2R + 1)/(2R + 2) = 5/6$ and is optimal.

A more general analysis can be undertaken by extending the isomorphism discussed above to a larger number of input and output particles N and M. In this case it is found that the QI-OPA amplification process $\hat{U}_U$ in each order of the decomposition into the parameter g corresponds to the $N \rightarrow M$ cloning process. Precisely, in this case $M \geq N$ output particles are detected over the output cloning mode $\mathbf{k}_1$. Correspondingly, $M - N$ particles are detected over the output anticloning mode $\mathbf{k}_2$. The cloning transformation is realized *a posteriori* in the sense that the output number M of copies is a random variable that is selected as the result of the measurement of the photon number in the anticloning beam (Simon, Weihs, and Zeilinger, 2000).

It appears clear, from the above analysis, that the effect of the input vacuum field which is necessarily injected in any universal optical amplifier is indeed responsible to reduce the fidelity of the quantum-cloning machines at hand. More generally, the vacuum field is in precise correspondence with, and must be interpreted as, the amount of QED vacuum fluctuations that determines the upper bounds to the fidelity determined by the structure of quantum mechanics.

The universal cloning was realized by exploiting the stimulated emission induced by a single photon by De Martini *et al.* (2002), Pelliccia *et al.* (2003), and De Martini, Pelliccia, and Sciarrino (2004) as shown in Fig. 3. There a spontaneous parametric downconversion process excited by the $-\mathbf{k}_p$ pump mode created single pairs of photons with equal wavelengths in entangled singlet states of linear polarization. One photon of each pair, emitted over $-\mathbf{k}_1$, was reflected by a spherical mirror into the crystal where it provided the $N = 1$ single-photon injection into the optical parametric amplifier excited by the pump beam associated with the backreflected mode $\mathbf{k}_p$. Hence the optimal cloning process was realized along the mode $\mathbf{k}_1$. A similar experiment has been reported by Lamas-Linares *et al.* (2002) where the single-photon initial qubit was implemented by a highly attenuated coherent-state beam.

B. Universal optimal NOT gate

The NOT gate, the transformation that maps any qubit onto the orthogonal qubit, i.e., onto its antipode on the Bloch sphere, has been recognized to be impossible to carry out according to the principles of quantum mechanics (Bechmann-Pasquinucci and Gisin, 1999). In fact, if $|\Psi\rangle = \alpha|0\rangle + \beta|1\rangle$ is a generic qubit, its antipode is generated by the time-reversal transformation $T|\Psi\rangle = |\Psi^{\perp}\rangle = \beta^*|0\rangle - \alpha^*|1\rangle$ such that $\langle\Psi \mid \Psi^{\perp}\rangle = 0$. As is well known T, being an antiunitary transformation, is not allowed by quantum mechanics: it may be expressed as $T = \sigma_y K$ with K being the transposition or phase conjugation map (Nielsen and Chuang, 2000). All this is at variance with the notion of classical information theory by which the NOT gate is the simplest operation to be performed exactly on any classical bit. The optimal approximation of the U-NOT gate maps N identical input qubits $|\phi\rangle$ into M optimally flipped ones in the state σ_{out} and achieves the fidelity

$$\mathcal{F}^{*}_{N\to M}(|\phi^{\perp}\rangle, \sigma_{\text{out}}) = \langle\phi^{\perp}|\sigma_{\text{out}}|\phi^{\perp}\rangle = \frac{N+1}{N+2}. \qquad (17)$$

We note that $\mathcal{F}^{*}_{N\to M}$ depends only on the number of the input qubits (Buzek, Hillery, and Werner, 1999; Gisin and Popescu, 1999; Bužek and Hillery, 2000). Indeed, the fidelity of the U-NOT gate is exactly the same as the optimal quantum estimation fidelity (Massar and Popescu, 1995). This means that the realization of this process is equivalent to a classical preparation of M identical flipped qubits following an approximate quantum estimation of N input states. Only this last operation is affected by noise, and in the limit $N \to \infty$ a perfect estimation of the input state is achieved, leading to the realization of an exact flipping operation.

We consider again the expression (15) of the output state of the optical parametric amplifier. The vector $|0, 1\rangle_2$ describes the state of the mode $\mathbf{k}_2$ with a single photon in the polarization state $|\Psi^{\perp}\rangle$. This state vector represents the flipped version of the input qubit on mode $\mathbf{k}_1$ and then the QI-OPA acts on the output mode $\mathbf{k}_2$ as a universal-NOT gate (De Martini *et al.*, 2002). We see that the flipped qubits described by the state vector $|0, 1\rangle_2$ on the right-hand sides of Eqs. (15) and (16) appear with different amplitudes corresponding to the ratio of probabilities $R^{*} = 2{:}1$. Note in Eqs. (15) and (16) that, by indicating by R the ratio of the probabilities of detecting two and one photon(s) in mode $\mathbf{k}_1$ only, we obtain $R = R^{*}$. In other words, the *same value* of the signal-to-noise ratio affects both cloning and U-NOT processes realized simultaneously in the two different output modes $\mathbf{k}_1$ and $\mathbf{k}_2$. The corresponding value of the U-NOT fidelity reads $\mathcal{F}^{*} = 2/3$ and is equal to the optimal one allowed by quantum mechanics (De Martini *et al.*, 2002).

A remarkable and somewhat intriguing aspect of the present process is that both processes of quantum cloning and the U-NOT gate are realized contextually by the same physical apparatus, by the same unitary transformation, and correspondingly by the same quantum logic network (De Martini, Pelliccia, and Sciarrino, 2004).

The relation between the cloning and the NOT operations has been discussed according to the conservation laws alone (van Enk, 2005). It was suggested that the close link existing between the limitations on cloning and NOT operations could express an as yet unexplored natural law. The results discussed above are general and hold in both the classical and quantum-mechanical worlds, for both optimal and suboptimal operations, and for bosons as well as fermions.

C. Optimal machines by symmetrization

Optimal quantum-cloning machines, although working probabilistically, have been demonstrated experimentally by a symmetrization technique (Irvine *et al.*, 2004; Ricci *et al.*, 2004; Sciarrino *et al.*, 2004a, 2004b). This approach to the probabilistic implementation of the N-to-M cloning process was first proposed by Werner (1998). It is based on the action of a projective operation on the symmetric subspace of the N input qubits and $M - N$ blank ancillas. This transformation assures the uniform distribution of the initial information in the overall system and guarantees that all output qubits are indistinguishable. To achieve the projection over the symmetric subspace we exploit the bosonic nature of photons, viz., the exchange symmetry of their overall wave function. In particular, we use a two-photon Hong-Ou-Mandel coalescence effect (Hong, Ou, and Mandel, 1987). In this process, two photons impinging simultaneously on a beam splitter (BS) from two different input modes have an enhanced probability of emerging along the same output mode (that is, *coalescing*), as long as they are indistinguishable. If the two photons are made distinguishable, e.g., by different encoding of their polarization or of any other degree of freedom, the coalescence effect vanishes. Now, if one of the two photons involved in the process is in a known input state to be cloned and the other is in a random one, the coalescence effect will enhance the probability that the two photons emerge from the beam splitter with the same quantum state. In other words, the symmetrization enhances the probability of a successful cloning detected at the output of the beam splitter.

Universal optimal quantum cloning based on the symmetrization technique was first demonstrated for the polarization-encoded qubit (Irvine *et al.*, 2004; Ricci *et al.*, 2004; Sciarrino *et al.*, 2004a, 2004b) and later reported for orbital angular-momentum-encoded qubits (Nagali *et al.*, 2009). Finally Nagali *et al.* (2010) reported the experimental realization of the optimal quantum cloning of four-dimensional quantum states, or ququarts, encoded in the (polarization + orbital angular momentum) degrees of freedom of photons (Marrucci *et al.*, 2011).

D. Phase-covariant optimal quantum cloning

In addition to the impossibility of universally cloning unknown qubits, there exists the impossibility of cloning subsets of qubits containing nonorthogonal states. This no-go theorem has been adopted to provide the security of cryptographic protocols such as the Bennett-Brassard 1984 (BB84) protocol (Gisin *et al.*, 2002). Recently state-dependent, nonuniversal, optimal cloning machines have been investigated where the cloner is optimal with respect to a given ensemble (Bruß *et al.*, 2000). This partial *a priori* knowledge of the state allows one to reach a larger fidelity than for universal cloning.

The simplest and most relevant case is represented by the covariant cloning under the Abelian group U(1) of phase rotations, the so-called phase-covariant cloning. There the information is encoded in the phase ϕ_i of the input qubit belonging to the equatorial plane i of the corresponding Bloch sphere. In this context the general state to be cloned may be expressed as $|\phi_i\rangle = (|\psi_i\rangle + e^{i\phi_i}|\psi_i^{\perp}\rangle)$ and $\{|\psi_i\rangle, |\psi_i^{\perp}\rangle\}$ is a convenient orthonormal basis (Bruß *et al.*, 2000). The values of the optimal fidelities $\mathcal{F}^{N\to M}_{\text{cov}}$ for the phase-covariant cloning machine were found by D'Ariano and Macchiavello (2003). Restricting the analysis to a single input qubit to be cloned, $N = 1$, into $M > 1$ copies, the cloning fidelity is found

$$\mathcal{F}^{1\to M}_{\text{cov}} = \frac{1}{2}\left(1 + \frac{M+1}{2M}\right)$$

for M assuming odd values, or

$$\mathcal{F}^{1\to M}_{\text{cov}} = \frac{1}{2}\left(1 + \frac{\sqrt{M(M+2)}}{2M}\right)$$

for M even. In particular, we have $\mathcal{F}_{\rm cov}^{1\to 2}=0.854$ and $\mathcal{F}_{\rm cov}^{1\to 3}=0.833$ to be compared with the corresponding figures valid for universal cloning: $\mathcal{F}_{\rm univ}^{1\to 2}=0.833$ and $\mathcal{F}_{\rm univ}^{1\to 3}=0.778$. It is worth noting the deep connection linking the phase-covariant cloning and the estimation of an equatorial qubit, that is, with the problem of finding the optimal strategy to estimate the value of the phase ϕ (Derka, Buzek, and Ekert, 1998). In general, for $M\to\infty$, $\mathcal{F}_{\rm cov}^{N\to M}\to\mathcal{F}_{\rm phase}^{N}$. In particular, we have $\mathcal{F}_{\rm cov}^{1\to M}=\mathcal{F}_{\rm phase}^{1}+1/4M$ with $\mathcal{F}_{\rm phase}^{1}=3/4$.

We briefly review different schemes which can be realized through the methods of quantum optics outlined above (Sciarrino and De Martini, 2007). We restrict our attention to the $1\to 3$ phase-covariant quantum-cloning machine as the corresponding scheme can be easily extended to the general case $1\to M$ for odd values of M. The phase-covariant cloner can be realized by adopting a QI-OPA working in a collinear configuration: see Fig. 1(c) (De Martini, 1998b). In this case the interaction Hamiltonian $\hat{\mathcal{H}}_{\rm PC}=i\chi\hbar(\hat{a}_H^\dagger\hat{a}_V^\dagger)+$ H.c. acts on a single output spatial mode $\mathbf{k}$. A fundamental physical property of $\hat{\mathcal{H}}_{\rm PC}$ consists of its rotational invariance under U(1) transformations, that is, under any arbitrary rotation around the z axis. Consider an injected single photon with polarization state $|\phi\rangle_{\rm in}=2^{-1/2}(|H\rangle+e^{i\phi}|V\rangle)=|1,0\rangle_k$, where $|m,n\rangle_k$ represents a product state with m photons of the mode $\mathbf{k}$ with polarization ϕ, and n photons with polarization $\phi^\perp$. The first contribution to the amplified state, $\sqrt{6}|3,0\rangle_k-\sqrt{2}e^{i2\phi}|1,2\rangle_k$, is identical to the output state

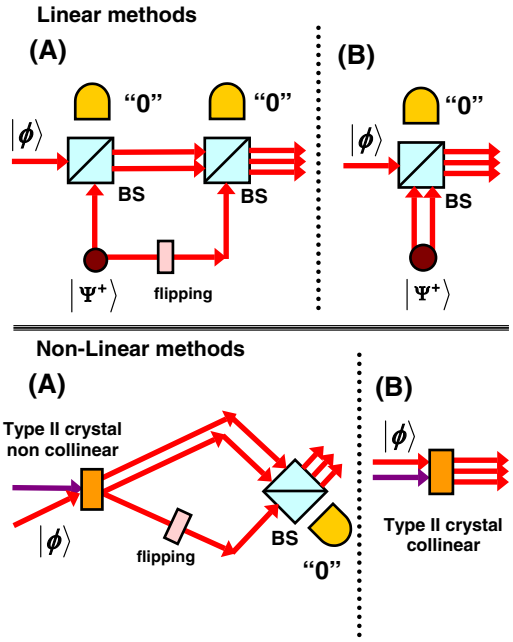

FIG. 4 (color online). Linear methods: (a) schematic diagram of the linear optics multiqubit symmetrization apparatus realized by a chain of interconnected Hong-Ou-Mandel interferometers; (b) symmetrization of the input photon and the ancilla polarization-entangled pairs. Nonlinear methods: (a) universal quantum cloning machine by optical parametric amplification, flipping by two wave plates and projection over the symmetric subspace; (b) collinear optical parametric amplification. From Sciarrino and De Martini, 2007.

obtained from a $1\to 3$ phase-covariant cloning. Indeed, the fidelity is found to be the optimal one $F^{1\to 3}=\frac{5}{6}$ (Sciarrino and De Martini, 2007). Notice the effect of the input vacuum field over the single $\mathbf{k}$ mode with polarization $\phi^\perp$ coupled to the phase-covariant optical amplifier. This vacuum contribution is indeed responsible for reducing the fidelity of the quantum-cloning machine.

Interestingly, the same overall state evolution can also be obtained at the output of a noncollinear QI-OPA together with a Pauli σ_Y operation and the projection of the three output photons over the symmetric subspace [see Fig. 4(a)]. This scheme was experimentally realized by the following method: the flipping operation on the output mode $\mathbf{k}_{\rm AC}$ was realized by means of two wave plates, while the physical implementation of the symmetrization projector on the three photon states was carried out by linearly superimposing the modes $\mathbf{k}_C$ and $\mathbf{k}_{\rm AC}$ on a BS and then by selecting the case in which the three photons emerged from the BS all in the same output mode $\mathbf{k}_{\rm PC}$ (Sciarrino and De Martini, 2005).

IV. PARAMETRIC AMPLIFICATION AND THE NO-SIGNALING THEOREM

Here we review the connections between the cloning process and the special theory of relativity according to which any signal carrying information cannot travel at a speed larger than the velocity of light in vacuum c. Even though quantum physics has marked nonlocal features due to the existence of entanglement, it has been found that a no-signaling theorem exists according to which one cannot exploit quantum entanglement between two spacelike-separated parties for faster-than-light communication (Maudlin, 2002). Several attempts to break this peaceful coexistence have been proposed, the most renowned one by Herbert in 1981 by the first laser-amplified superluminal hookup (FLASH) machine (Herbert, 1982). The publication of this proposal, based on a cloner machine applied to an entangled state of two spacelike-distant particles A and B, was followed by a debate that eventually stimulated the formulation of the no-cloning theorem (Wootters and Zurek, 1982).

The setup proposed by Herbert is shown in Fig. 5. If one observer Bob, by measuring the particle B could distinguish between different state mixtures that have been prepared by the distant observer Alice by measuring the particle A, then quantum nonlocality could be used for signaling. Precisely, consider the following: Alice and Bob share two polarization-entangled photons A and B generated by a common source. Alice detects her photon polarization with the detectors D_φ^A and $D_{\varphi\perp}^A$ in either the basis $\{\vec{\pi}_\pm=2^{-1/2}(\vec{\pi}_V\pm\vec{\pi}_H)\}$ or $\{\vec{\pi}_R=2^{-1/2}(\vec{\pi}_H+i\vec{\pi}_V),\vec{\pi}_L=2^{-1/2}(\vec{\pi}_V-i\vec{\pi}_H)\}$, where $\vec{\pi}_H$ and $\vec{\pi}_V$ are linear horizontal and vertical polarization, respectively. If Bob could guess with a probability larger than $\frac{1}{2}$ the basis chosen by Alice, superluminal signaling would be established. It was recognized that this is impossible if the experiment involves two single particles. However, Herbert thought that Bob could make a new kind of measurement involving the amplification of the received signal B through a nonselective laser gain tube, viz., a universal (polarization-independent) amplifier. The amplified photon beam is split by an optical BS, so Bob can perform on one of the two output

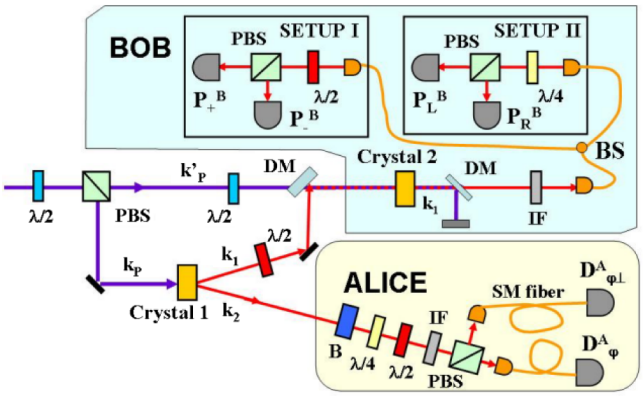

FIG. 5 (color online). Configuration of the quantum-injected optical parametric amplifier. The SPDC quantum injector (crystal 1) is provided by a type-II generator of polarization-entangled photon pairs. From De Angelis *et al.*, 2007.

channels of the BS a measurement on half of the cloned particles by an apparatus tuned on the basis $\{\vec{\pi}_{\pm}\}$ which records the signal $I^B_{\pm}$. Simultaneously, he could record on the other BS output channel the signals $I^B_{R/L}$ by an apparatus tuned on the basis $\{\vec{\pi}_R, \vec{\pi}_L\}$. In that way he could guess the right preparation basis carried out by Alice on particle A.

In order to test Herbert's scheme a careful theoretical and experimental analysis of the output field was carried out with an emphasis on fluctuations and correlations (De Angelis *et al.*, 2007). Precisely, Herbert's scheme was reproduced by the optical parametric amplification of a single photon of an entangled pair into an output field involving 5×10^3 photons (see Fig. 5). Unexpected and peculiar field correlations among the cloned particles preventing any violation of the no-signaling conditions have been found. Precisely, it was found that the limitations implied by a complete quantum-cloning theory are not restricted to the bounds on the cloning fidelity but also greatly affect the high-order correlations existing among the different clones. In fact, in spite of a reduced fidelity, noisy but separable, i.e., noncorrelated, copies would lead to a perfect state estimation for $g \to \infty$ and hence to a real possibility of superluminal communication. However, surprisingly enough particles produced by any optimal cloning machine are highly interconnected and the high-order correlations are actually responsible for preventing any possibility of faster-than-light communication (Demkowicz-Dobrzanski, 2005; Bae and Acín, 2006; De Angelis *et al.*, 2007). Recently Zhang (2011) investigated the wave packet propagation of a single photon and showed experimentally in a conclusive way that the single-photon speed is limited by c.

V. EXPERIMENTAL MACROSCOPIC QUANTUM SUPERPOSITION BY MULTIPLE CLONING OF SINGLE-PHOTON STATES

A. Generation and detection of multiparticle quantum superpositions

This section describes the optical parametric amplification of a single photon in the high-gain regime to experimentally investigate how the information initially contained in its polarization state is distributed over a large number of particles. In particular, we analyze how the coherence properties of the input state are transferred to the mesoscopic output field.

We consider the scenario in which a single-particle qubit $|\psi\rangle_B = \alpha|\phi\rangle_B + \beta|\phi^{\perp}\rangle_B$, with $|\alpha|^2 + |\beta|^2 = 1$, injected in a three-wave optical parametric amplifier (Yariv, 1989), is transformed by the unitary QI-OPA operation into a corresponding MQS:

$$|\Phi\rangle_B = \alpha|\Phi^{\phi}\rangle_B + \beta|\Phi^{\phi\perp}\rangle_B. \tag{18}$$

The multiparticle states, or macrostates, whose detailed expression is reported in Eq. (10), bear peculiar properties that deserve some comments. The macrostates $|\Phi^{\phi}\rangle_B$ and $|\Phi^{\phi\perp}\rangle_B$ are orthonormal and exhibit observables bearing macroscopically distinct average values. Precisely, the average number of photons associated with the polarization mode $\vec{\pi}_{\phi}$ is $\bar{m} = \sinh^2 g$ for $|\Phi^{\phi\perp}\rangle_B$, and $(3\bar{m} + 1)$ for $|\Phi^{\phi}\rangle_B$. For the π mode $\vec{\pi}_{\phi\perp}$, orthogonal to $\vec{\pi}_{\phi}$, these values are interchanged between the two states. On the other hand, as shown by De Martini (1998a), by changing the representation basis from $\{\vec{\pi}_{\phi}, \vec{\pi}_{\phi\perp}\}$ to $\{\vec{\pi}_H, \vec{\pi}_V\}$, the same macrostates $|\Phi^{\phi}\rangle_B$ and $|\Phi^{\phi\perp}\rangle_B$ are found to be again quantum superpositions of two orthonormal states $|\Phi^H\rangle_B$ and $|\Phi^V\rangle_B$, differing by a single quantum. This unexpected and quite peculiar combination, i.e., a large difference of a measured observable when the states are expressed in one basis and a small Hilbert-Schmidt distance of the same states when expressed in another basis, turned out to be a fundamental property that renders the coherence properties of the system robust toward the coupling with the environment. This is discussed later in Sec. VII.

We first briefly review the adopted optical system, making reference to the experimental layout shown by the sketch in Fig. 1(c), or by the equivalent, more detailed Fig. 6 (Caminati, De Martini, and Sciarrino, 2006; Nagali *et al.*, 2007; De Martini, Sciarrino, and Vitelli, 2008). An entangled pair of two photons in the singlet state $|\psi^-\rangle_{A,B} = 2^{-1/2}(|H\rangle_A|V\rangle_B - |V\rangle_A|H\rangle_B)$ was produced through SPDC by the BBO crystal 1 (C1) pumped by a (weak) pulsed ultraviolet pump beam (see Fig. 6). There the labels A and B refer to particles associated, respectively, with the two output spatial modes $\mathbf{k}_A$ and $\mathbf{k}_B$ of the SPDC generated by C1. In the experiment the three spatial modes involved in the injected parametric interaction were carefully selected by adopting single-mode fibers. Consequently, by virtue of Eqs. (1) and (2), a three-wave, collinear phase-matching condition was realized leading to a lossless amplification process.

The single-photon qubit on mode $\mathbf{k}_A$ of Fig. 6 [i.e., $\mathbf{k}_2$ in Fig. 1(c)] was sent to a polarizing beam splitter (PBS) whose output modes were coupled to two single-photon detectors. In the first experiment, these two detectors were simply connected as to merely identify the emission of A (and of B) without any effective polarization measurement on A. In other words, the two detectors acted as the single detector unit D_2 of the simplified Fig. 1(c) by supplying a single electronic trigger signal for the overall experiment in correspondence with the emission of any entangled couple A and B emitted by C1. By virtue of this trigger signal the overall measurement

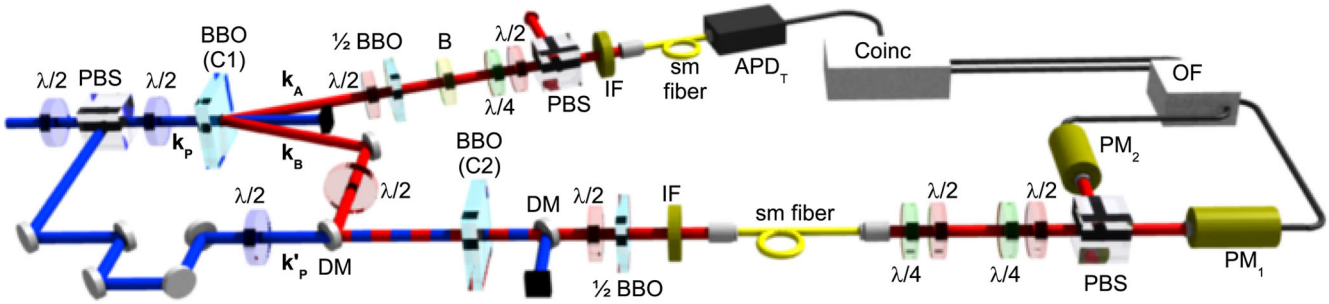

FIG. 6 (color online). Scheme of the experimental setup. The main ultraviolet laser beam provides the excitation field beam at $\lambda_P = 397.5$ nm. A type-II BBO crystal (crystal 1: C1) generates a pair of photons with $\lambda = 795$ nm. The photon belonging to $\mathbf{k}_B$, together with the pump laser beam $\mathbf{k}'_p$, is fed into a high-gain optical parametric amplifier consisting of a crystal 2 (C2), cut for collinear type-II phase matching. The residual UV pump beam and the amplified quantum states are spectrally separated by exploiting a dichroic mirror (DM). Measurement apparatus: the field is analyzed by two photomultipliers (PM_1 and PM_2) and then discriminated through an O-filter device (OF), whose action is described in the text. From De Martini, Sciarrino, and Vitelli, 2008.

of the MQS $|\Phi\rangle_B$ could be considered heralded by, i.e., measured in coincidence with, any photon A measured on mode $\mathbf{k}_A$. Accordingly, no bipartite micro-macro entanglement was detectable (De Martini, 1998b; De Martini, Sciarrino, and Vitelli, 2008).

The single-particle qubit $|\psi\rangle_B = 2^{-1/2}(|H\rangle_B - |V\rangle_B)$ associated with particle B prepared in the superposition state of the polarization state was then injected, together with a very intense laser pulsed pump beam into the main optical parametric amplifier consisting of a second BBO crystal 2 (C2): Fig. 8. The crystal C2 was oriented for *collinear operation*, i.e., emitting pairs of amplified photons over the same output spatial mode supporting two orthogonal polarization, respectively horizontal and vertical modes. The high-gain parametric amplification provided by the crystal C2 transformed the single-particle qubit $|\psi\rangle_B$ into the corresponding multiparticle MQS $|\Phi\rangle_B = 2^{-1/2}(|\Phi^{\phi}\rangle_B - |\Phi^{\phi\perp}\rangle_B)$. This MQS, composed of $M \approx 5 \times 10^4$ photons, was analyzed by a polarization analyzer $[A(\varphi)]$ coupled through a PBS to two high-gain photomultipliers with detection efficiency $\simeq 5\%$. The number of photons M and the relative uncertainty have been estimated via the parametric gain g experimentally derived by measuring how the number of emitted photons increases with the pumping power (Caminati *et al.*, 2006b; Nagali *et al.*, 2007). The device $A(\varphi)$ composed of an optical rotator and a birefringent plate analyzed the MQS $|\Phi\rangle_B$ in a rotating base characterized by a single φ phase. More details are given by De Martini (1998b).

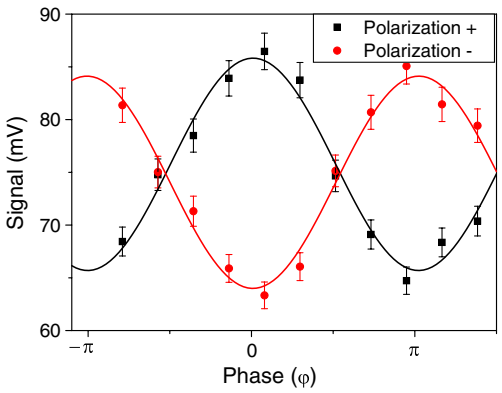

FIG. 7 (color online). Average signal vs the phase of the input qubit. From Nagali *et al.*, 2007.

The sinusoidal behavior shown by the detected experimental interference-fringe pattern reported in Fig. 7 as a function of φ offers a visual realization of the original 1935 pictorial argument by Schrödinger (1935). These interference-fringe patterns show how the coherent quantum superposition properties of the one photon input state can be transferred to the mesoscopic output, involving a very large number of photon particles. There the minima and the maxima of the patterns, e.g., shown by Fig. 7, can be attributed to the dead or alive conditions of the celebrated Schrödinger cat, i.e., of the macrosystem. Similar MQS interference-fringe patterns arising in different experiments have been obtained, e.g., as shown by Fig. 9 and by Fig. 4 of De Angelis *et al.* (2007). As mentioned, all MQS results were obtained at room temperature, thus defying the phase-disrupting decoherence process that generally affects this kind of experiment. However, we see that the observation of other sophisticated quantum effects such as the entanglement correlations within micro-macro systems requires not only a system well protected against environmental decoherence, but also a sufficient measurement resolution. We show also that, in spite of the reported successful evidence of the MQS realization, the

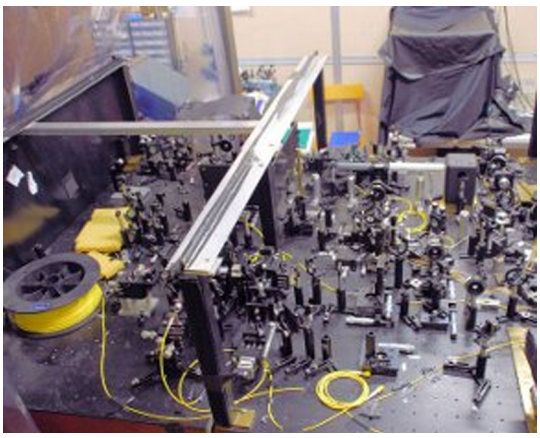

FIG. 8 (color online). The experimental apparatus adopted for the amplification of entangled pairs of photons (Quantum Optics Group, Dipartimento di Fisica, Sapienza Universita di Roma).

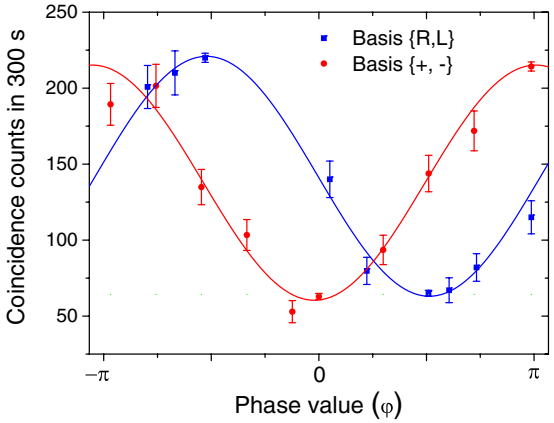

FIG. 9 (color online). Coincidence counts $[L_B; D_A]$ vs the phase of the injected qubit for the diagonal (circles) and circular (squares) polarization bases. From De Martini, Sciarrino, and Vitelli, 2008.

measurement of bipartite micro-macro entanglement with very large M meets severe experimental problems, owing to a newly discovered multiparticle efficiency loophole (Sekatski *et al.*, 2009). However, by a different quantum tomographic test within a deliberate attenuation experiment carried out in a noncollinear configuration, the achievement of bipartite micro-macro entanglement was demonstrated for a limited number of QI-OPA-generated particles: $M \leq 12$ (De Martini, Sciarrino, and Secondi, 2005) The last experiment, demonstrating the achievement of bipartite micro-macro entanglement as well as of the MQS condition, is discussed in Secs. VI and IX.

VI. MICRO-MACRO SYSTEM: HOW TO DEMONSTRATE ENTANGLEMENT

Owing to the close similarity existing between the QI-OPA scheme shown in Fig. 1(c) and the well-known Einstein-Podolsky-Rosen (EPR) scheme it may be argued that the nonlocal separability between the single-photon qubit $|\psi^-\rangle_{A,B} = 2^{-1/2}(|H\rangle_A|V\rangle_B - |V\rangle_A|H\rangle_B)$ emitted over the output mode $\mathbf{k}_B$ and the macrostate emitted over $\mathbf{k}_A$ could be demonstrated experimentally (Caminati, De Martini, and Sciarrino, 2006). Formally, this endeavor consists of a demonstration of the existence of the entangled state connecting the two micro-macro systems A and B:

$$|\Psi^-\rangle_{AB} = \frac{1}{\sqrt{2}}(|\phi\rangle_A|\Phi^{\phi_\perp}\rangle_B - |\phi_\perp\rangle_A|\Phi^{\phi}\rangle_B). \tag{19}$$

There the output macrostate is expressed by $|\Phi^\phi\rangle = \hat{U}_{\mathrm{PC}}|\phi\rangle$, where $|\phi\rangle$ labels the injection of a single-photon state as in Eq. (7).

Such a demonstration consists of a complete physical achievement of the 1935 Schrödinger cat program. In the following sections different theoretical and experimental approaches are briefly discussed. In particular, an ambitious attempt in this direction was undertaken with a high-gain QI-OPA method generating a macrostate consisting of nearly $M = 10^4$ photons. The experimental layout was similar to the one described in Sec. V but adopted a different, sophisticated processing of the signals generated by the particle detectors (De Martini, Sciarrino, and Vitelli, 2008). However, it was soon realized that a conclusive test of micro-macro entanglement for a very large number of particles could be achieved successfully only by adoption of linear photomultipliers featuring a large detection efficiency $\eta \lesssim 1$, a condition not made available by the present technology (Sekatski *et al.*, 2009). This is but the effect of a new form of the well-known detection loophole which affects in general all nonlocality tests and is found to worsen for an increasing number M of detected particles. However, as stated, in spite of all these problems a conclusive experimental demonstration of micro-macro entanglement has been realized by a quantum tomographic method for a limited number of multiparticle quantum superpositions $M \lesssim 12$, as we describe in the next section.

A. Extracted two-photon density matrices

A feasible approach for the analysis of multiphoton fields is based on the deliberate attenuation of the analyzed system up to the single-photon level (Eisenberg *et al.*, 2004). In this way, standard single-photon techniques and criteria can be used to investigate the properties of the field. The verification of the bipartite entanglement in the high-loss regime is evidence of the presence of entanglement before attenuation, on the premise that no entanglement can be generated by any local operations, including lossy attenuation. The attenuation method has been applied to the micro-macro system, realizing by a quantum tomographic method the experimental proof of the presence of entanglement between the single-photon state of mode $\mathbf{k}_A$ and the multiphoton state with $M \lesssim 12$ of mode $\mathbf{k}_B$ generated through the process of parametric amplification in a universal cloning configuration (see Fig. 6). The theory of this experiment is considered once again in more detail in Sec. IX (De Martini, Sciarrino, and Secondi, 2005; Caminati *et al.*, 2006a). Unfortunately, such an approach could be applied only for a very limited number M, since in practice unavoidable experimental imperfections quickly wash out any evidence of entanglement (Spagnolo *et al.*, 2010).

B. Pseudospin operators

We now address a different criterion to verify the bipartite entanglement between modes $\mathbf{k}_A$ and $\mathbf{k}_B$. We adopt the standard Pauli operators for the single-photon polarization state of mode $\mathbf{k}_A$. We introduce a formalism useful to associate the amplified multiparticle field in mode $\mathbf{k}_B$ to a macroqubit. Through the amplification process the spin operators $\hat{\sigma}_i$ of the single photon evolve into the macrospin operators $\hat{\Sigma}_i$ for the many-particle system $\hat{\Sigma}_i = \hat{U}\hat{\sigma}_i\hat{U}^\dagger = |\Phi^{\psi i}\rangle\langle\Phi^{\psi i}| - |\Phi^{\psi i\perp}\rangle\langle\Phi^{\psi i\perp}|$. The operators $\{\hat{\Sigma}_i\}$ satisfy the same commutation rules as the single-particle $\frac{1}{2}$-spin $[\hat{\Sigma}_i, \hat{\Sigma}_j] = \varepsilon_{ijk}2i\hat{\Sigma}_k$, where ε_{ijk} is the Levi-Cività tensor density. Hence the generic state $\alpha|\Phi^H\rangle_B + \beta|\Phi^V\rangle_B$ can be handled as a qubit in the Hilbert space H_B spanned by $\{|\Phi^H\rangle_B, |\Phi^V\rangle_B\}$. To test whether the output state is entangled, one should measure the correlation between the single-photon spin operator $\hat{\sigma}_i^A$ on mode $\mathbf{k}_A$ and the macrospin operator $\hat{\Sigma}_i^B$ on mode $\mathbf{k}_B$. We then adopt the criteria for two-qubit bipartite systems based on the spin correlation. We define the visibility $V_i = |\langle\hat{\Sigma}_i^B \otimes \hat{\sigma}_i^A\rangle|$, a

parameter which quantifies the correlation between the systems A and B. The value $V_i = 1$ corresponds to perfect anticorrelation, while $V_i = 0$ expresses the absence of correlation. The following upper bound criterion for a separable state holds (Eisenberg *et al.*, 2004): $S = \sum_i V_i \leq 1$. In order to measure the expectation value of $\hat{\Sigma}_i^B$, a discrimination among the pairs of states $\{|\Phi^{\psi i}\rangle, |\Phi^{\psi i\perp}\rangle\}$ for the three different polarization bases 1, 2, and 3 is required. Consider the two macrostates $|\Phi^+\rangle$ and $|\Phi^-\rangle$. Perfect discrimination can be achieved by identifying whether the number of photons in the $\mathbf{k}_B$ mode with polarization $\vec{\pi}_+$ is even or odd. Asnoted, this requires the detection of the mesoscopic field by a photon-number-resolving detector operating with an overall quantum efficiency $\eta \approx 1$, a device not yet made available by the present technology. Here we face the problem of detecting correlations by performing a coarse-grained measurement process.

C. Correlation measurements via orthogonality filter

In order to implement a measurement with high discrimination, a new method has been adopted, viz., the O-filter (OF)-based strategy. This method is based on a probabilistic discrimination of the macrostates $|\Phi^\phi\rangle$ and $|\Phi^{\phi_\perp}\rangle$, which exploits the macroscopic features present in their photon-number distributions (Nagali *et al.*, 2007). This measurement is implemented by an intensity measurement carried out with multiphoton linear detectors in the $\{\vec{\pi}_i, \vec{\pi}_i^\perp\}$ basis, followed by an electronic processing of the recorded signal. If $n_\pi - m_{\pi_\perp} > k$, the $(+1)$ outcome is assigned to the event, if $m_{\pi_\perp} - n_\pi > k$ the (-1) outcome is assigned to the event. If $|n_\pi - m_{\pi_\perp}| < k$, an inconclusive outcome (0) is assigned to the event.

Experimentally the photon is detected in mode $\mathbf{k}_A$ adopting single-photon detectors and the multiphoton field of mode $\mathbf{k}_B$ with photomultipliers and an O filter. The experimental fringe patterns shown in Fig. 9 were obtained by adopting the common analysis basis $\{\vec{\pi}_R, \vec{\pi}_L\}$ with a filtering probability $\simeq 10^{-4}$. In this case the average visibility was found to be $V_2 = (54.0 \pm 0.7)\%$. A similar oscillation pattern was obtained in the basis $\{\vec{\pi}_+, \vec{\pi}_-\}$, leading to $V_3 = (55 \pm 1)\%$. Since $V_1 > 0$ always, the experimental result $S = V_2 + V_3 = (109.0 \pm 1.2)\%$ implies the violation of the separability criterion introduced above. However, a careful analysis of the implications of discarding part of the data obtained via the OF measurement should be addressed.

The state after losses is no longer a macroqubit existing in a two-dimensional Hilbert space, but in general it is represented by a density matrix $\hat{\rho}_\eta^\phi$. A detailed discussion of the properties of the macrostates after losses in both the Fock space and the phase space was reported by De Martini, Sciarrino, and Spagnolo (2009a) and Spagnolo *et al.* (2009, 2010). In general, the probabilistic detection method described above can be adopted to infer the active generation before losses of a macrostate $|\Phi^\phi\rangle$ or $|\Phi^{\phi_\perp}\rangle$, by exploiting the information encoded in the imbalance of the number of particles present in the state after losses $\hat{\rho}_\eta^\phi$. Hence the adopted entanglement criterion allows one to infer the presence of bipartite micro-macro entanglement present before losses, under a specific assumption (De Martini, Sciarrino, and Vitelli, 2008). This point was discussed extensively by Sekatski *et al.* (2009, 2010), who showed that any loss of data allows the formulation of a kind of detection loophole that impairs the success of the entanglement demonstration. We recall that it has been known for at least four decades that a general detection loophole exists in the refutation of local realistic theories and is the source of skepticism about the definitiveness of all experiments dealing with single-particle Bell inequality violations. In fact, as claimed repeatedly by himself, because of the absence of an experimental confirmation of the fair-sampling assumption or of a plausible equivalent one, all experimental tests of Bell's inequality can today be interpreted in large areas of the scientific community as merely good indications of the real existence of quantum nonlocality (Greenberger, 1986; Bell, 1987; Maudlin, 2002). However, it is also well known that the detection loophole can be closed for single-particle Bell's inequality experiments by the adoption of detectors with efficiency as large as $\eta \geq 85\%$ (Eberhard, 1993). Unfortunately, our results show that an even larger value of η is required to demonstrate micro-macro entanglement in multiparticle systems. A thorough analysis of the micro-macro entanglement was carried out by Spagnolo *et al.* (2010), demonstrating that *a priori* knowledge of the system that generates the micro-macro pair is necessary to exclude a class of separable states that can reproduce the obtained experimental results (Pomarico *et al.*, 2011). In conclusion, the genuine unbiased demonstration of bipartite micro-macro entanglement, i.e., in the absence of any *a priori* assumption, is still an open experimental challenge when a very large number M of particles are involved.

D. Effects of coarse-grained measurement

Recently Raeisi, Sekatski, and Simon (2011) analyzed the effects of coarse graining in photon-number measurements on the observability of micro-macro entanglement that is created by greatly amplifying one photon from an entangled pair. They compared the results obtained for a unitary quantum cloner, which generates micro-macro entanglement, and for a measure-and-prepare cloner, which produces a separable micro-macro state. Their approach demonstrates that the distance between the probability distributions of results for the two cloners approaches zero for a fixed moderate amount of coarse graining. Once again, this proves that the detection of micro-macro entanglement becomes progressively harder as the system's size increases (Raeisi, Sekatski, and Simon, 2011).

As an alternative approach to demonstrate the micro-macro entanglement, Raeisi, Tittel, and Simon (2012) proposed a scheme where a photon is first cloned using stimulated parametric downconversion, making many optimal copies, and then the cloning transformation is inverted, regenerating the original photon while destroying the copies. Focusing on the case where the initial photon is entangled with another photon, Raeisi, Tittel, and Simon (2012) studied the conditions under which entanglement can be proven in the final state. This proposed experiment provides a clear demonstration that quantum information is preserved in phase-covariant quantum cloning, but again one photon should be lost between the

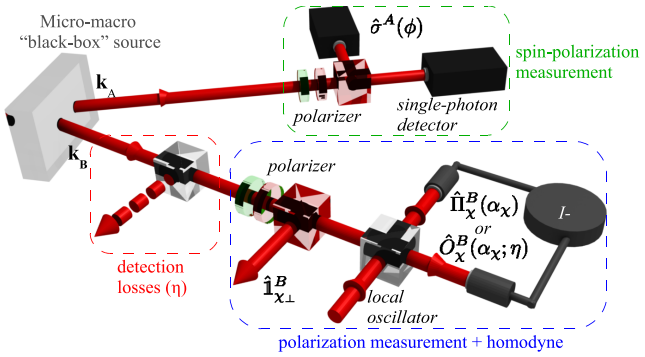

FIG. 10 (color online). Hybrid nonlocality and entanglement test on an optical microscopic-macroscopic state generated by a black box. The single-photon mode $\mathbf{k}_A$ is measured by a polarization detection apparatus, while the multiphoton mode $\mathbf{k}_B$ undergoes both polarization and homodyne measurements.

cloning trasformation and the following inversion process. The experimental reversion of the optimal quantum cloning and flipping processes was reported by Sciarrino, Secondi, and De Martini (2006). There, the combination of linear and nonlinear optical methods was exploited to implement a scheme that, after the cloning transformation, restores the original input qubit in one of the output channels, by using local measurements, classical communication, and feedforward. This nonlocal method demonstrated how the information on the input qubit can be restored after the cloning process.

E. Hybrid criteria

Recently Spagnolo *et al.* (2011) analyzed a hybrid approach to the experimental assessment of the genuine quantum features of a general system consisting of microscopic and macroscopic parts (see Fig. 10). They inferred the presence of entanglement by combining dichotomic measurements on a bidimensional system and phase-space inference through the Wigner distribution associated with the macroscopic component of the state. As a benchmark, the method was adopted to investigate the feasibility of the entanglement demonstration in a bipartite-entangled state composed of a single-photon and a multiphoton field. This analysis shows that, under ideal conditions, maximal violation of a Clauser-Horne-Shimony-Holt inequality is achievable regardless of the number of photons M in the macroscopic part of the state. The problems arising in the detection of entanglement when losses and detection inefficiency are included can be overcome by the use of a hybrid entanglement witness that allows efficient correction for losses in the few-photon regime. This analysis elicits further interest in the identification of a suitable test in the high-loss and large-photon-number region and paves the way toward an experimentally feasible demonstration of the properties of entanglement affecting a quite interesting class of states lying at the very border between the quantum and classical domains.

VII. RESILIENCE TO DECOHERENCE OF THE AMPLIFIED MULTIPARTICLE STATE

In this section we discuss the resilience to decoherence of the quantum states generated by optical parametric amplification of a single-photon qubit. The basic tools of this investigation are provided by two coherence criteria expressed by De Martini, Sciarrino, and Spagnolo (2009a, 2009b). There the Bures distance (Bures, 1969; Hubner, 1992; Jozsa, 1994),

$$\mathcal{D}(\hat{\rho},\hat{\sigma}) = \sqrt{1-\sqrt{\mathcal{F}(\hat{\rho},\hat{\sigma})}}, \tag{20}$$

where $\mathcal{F}$ is a quantum fidelity, has been adopted as a measure to quantify (I) the *distinguishability"* between two quantum states $\{|\phi_1\rangle, |\phi_2\rangle\}$ and (II) the *degree of coherence*, i.e., the superposition visibility, of their MQS $|\phi^+\rangle = 2^{-1/2}(|\phi_1\rangle \pm |\phi_2\rangle)$. These criteria were chosen according to the following considerations: (I) The distinguishability, i.e., the degree of orthogonality, represents the maximum discrimination between two quantum states achievable within a measurement. (II) The visibility between the superpositions $|\phi^+\rangle$ and $|\phi^-\rangle$ depends exclusively on the relative phase of the component states $|\phi_1\rangle$ and $|\phi_2\rangle$. Consider two orthogonal superpositions $|\phi^\pm\rangle$: $\mathcal{D}(|\phi^+\rangle, |\phi^-\rangle) = 1$. In the presence of decoherence the state evolves according to a phase-damping channel $\mathcal{E}$, the relative phase between $|\phi_1\rangle$ and $|\phi_2\rangle$ progressively randomizes, and the superpositions $|\phi^+\rangle$ and $|\phi^-\rangle$ approach an identical fully mixed state leading to $\mathcal{D}(\mathcal{E}(|\phi^+\rangle), \mathcal{E}(|\phi^-\rangle)) = 0$. The physical interpretation of $\mathcal{D}(\mathcal{E}(|\phi^+\rangle), \mathcal{E}(|\phi^-\rangle))$ as visibility is legitimate insofar as the component states of the corresponding superposition $|\phi_1\rangle$ and $|\phi_2\rangle$ may be defined, at least approximately, as *pointer* states or *einselected* states (Zurek, 2003). Within the set of eigenstates characterizing the system under investigation, the pointer states are defined as those that are less affected by the external noise and that are highly resilient to decoherence.

We now compare the resilience properties of the different classes of quantum states after propagation over a lossy channel $\mathcal{E}$. This one is modeled by a linear BS with transmittivity T and reflectivity $R = 1 - T$, acting on a state $\hat{\rho}$ associated with a single BS input mode. We first analyze the behavior of the coherent states and their superpositions. The investigation of Glauber's states leading to the α-MQS case (Schleich, Pernigo, and Le Kien, 1991) $|\Phi_{\alpha\pm}\rangle = \mathcal{N}^{-1/2}(|\alpha\rangle \pm |-\alpha\rangle)$ in terms of the pointer states $|\pm\alpha\rangle$ leads to the closed-form result $\mathcal{D}(\mathcal{E}(|\Phi_{\alpha+}\rangle), \mathcal{E}(|\Phi_{\alpha-}\rangle)) = \sqrt{1-\sqrt{1-e^{-4R|\alpha|^2}}}$. This is plotted in Fig. 11 (dashed line) as a function of the average number of lost photons $x \equiv R\langle n\rangle$. Note that the value of $\mathcal{D}(\mathcal{E}(|\Phi_{\alpha+}\rangle), \mathcal{E}(|\Phi_{\alpha-}\rangle))$ drops from 1 to 0.095 upon loss of only one photon $x = 1$, in other words, any superposition of α states. $|\Phi_{\alpha\pm}\rangle = \mathcal{N}^{-1/2}(|\alpha\rangle \pm |-\alpha\rangle)$ exhibits a fast decrease in its coherence, i.e., in its visibility and distinguishability, while the related components $|\pm\alpha\rangle$, i.e., the pointer states (Zurek, 2003), remain distinguishable until all photons of the state are depleted by the BS.

We now analyze the behavior of the amplified multiphoton states by the QI-OPA apparatus described in the previous sections. An EPR pair $|\psi^-\rangle = 2^{-1/2}(|H\rangle_A|V\rangle_B - |V\rangle_A|H\rangle_B)$ is generated in the first nonlinear crystal (see Fig. 6). By analyzing and measuring the polarization of the photon associated with the mode $\mathbf{k}_A$, the photon in mode $\mathbf{k}_B$ is prepared in the polarization qubit $|\psi\rangle_B = \cos(\theta/2)|H\rangle_B + e^{i\phi}\sin(\theta/2)|V\rangle_1$. Then, the single photon is injected into the amplifier simultaneously with the strong UV pump beam $\mathbf{k}'_P$. We analyze the two configurations of the apparatus leading,

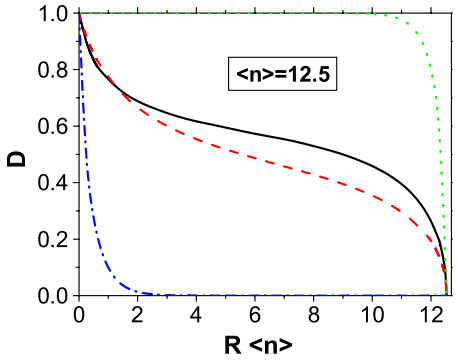

FIG. 11 (color online). Bures distance for various classes of MQSs for $\langle n\rangle = 12.5$. The lower dash-dotted curve corresponds to $\mathcal{D}(\mathcal{E}(|\phi^+\rangle), \mathcal{E}(|\phi^-\rangle))$, while the upper dotted curve is relative to the distinguishability $\mathcal{D}(\mathcal{E}(|\alpha^+\rangle), \mathcal{E}(|\alpha^-\rangle))$. The solid curve corresponds to the MQS generated by phase-covariant cloning $\mathcal{D}(\mathcal{E}(|\Phi^+_{PC}\rangle), \mathcal{E}(|\Phi^-_{PC}\rangle))$. From De Martini, Sciarrino, and Spagnolo, 2009a, 2009b. The dashed curve corresponds to the universal-cloning-based MQS $\mathcal{D}(\mathcal{E}(|\Phi^+_U\rangle), \mathcal{E}(|\Phi^-_U\rangle))$. From Spagnolo, Sciarrino, and De Martini, 2010.

as noted, to two different regimes of quantum cloning: the phase covariant and the universal.

A. Phase-covariant optimal quantum-cloning machine

We numerically evaluated the distinguishability of $\{|\Phi^{+,-}_{\rm PC}\rangle\}$ through the distance $\mathcal{D}(\mathcal{E}(|\Phi^+_{\rm PC}\rangle), \mathcal{E}(|\Phi^-_{\rm PC}\rangle))$ (see Fig. 11). Consider the MQS of the macrostates $|\Phi^+_{\rm PC}\rangle$, $|\Phi^-_{\rm PC}\rangle$: $|\Phi^{R/L}_{\rm PC}\rangle = (\mathcal{N}_\pm/\sqrt{2})(|\Phi^+_{\rm PC}\rangle \pm i|\Phi^-_{\rm PC}\rangle)$. Because of the linearity of the amplification process and by virtue of the phase covariance of the process (De Martini, Sciarrino, and Spagnolo, 2009a, 2009b),

$$\mathcal{D}(|\Phi^R_{\rm PC}\rangle, |\Phi^L_{\rm PC}\rangle) = \mathcal{D}(|\Phi^+_{\rm PC}\rangle, |\Phi^-_{\rm PC}\rangle). \tag{21}$$

These equations can be assumed as the theoretical conditions assuring the same behavior for any quantum MQS state generated by the QI-OPA in the collinear configuration: they identify the equatorial set of the Bloch sphere as a privileged set resilient to losses of Hilbert subspace. The *visibility* of the state $|\Phi^{R/L}_{\rm PC}\rangle$ was evaluated numerically by analyzing the Bures distance as a function of x (see Fig. 11). Note that for small values of x the decay of $\mathcal{D}(x)$ is far slower than for the coherent α-MQS case.

B. Universal optimal quantum-cloning machine

We now investigate the resilience to decoherence of the MQS generated by the universal optimal quantum-cloning machine (Spagnolo, Sciarrino, and De Martini, 2010). At variance with the phase-covariant amplifier, the output states do not exhibit a comb structure in their photon-number distributions. In agreement with the universality property of the source, the Bures distance between the MQS states $|\Phi^{1\psi}_U\rangle = \cos(\theta/2)|\Phi^{1H}_U\rangle + e^{i\phi}\sin(\theta/2)|\Phi^{1V}_U\rangle$ and $|\Phi^{1\psi_\perp}_U\rangle$ is independent of the choice of (θ, ϕ):

$$\mathcal{D}(\hat\rho^{1\psi}_U, \hat\rho^{1\psi_\perp}_U) = \mathcal{D}(\hat\rho^{1\psi'}_U, \hat\rho^{1\psi'_\perp}_U) \tag{22}$$

for any basis $\{\vec\pi_\psi, \vec\pi_{\psi'}\}$. The larger symmetry of the latter identifies a larger Hilbert space of macroscopic quantum superpositions resilient to decoherence, corresponding to the complete polarization Bloch sphere. The cost of this larger symmetry is a lower Bures distance in the universal with respect to the phase-covariant case. This represents an expected tradeoff in similar cases, e.g., it parallels the well-known increase of cloning fidelity due to the reduced size of the Hilbert subspace in the case of phase covariance.

C. Effective size of the multiparticle superposition

Recent experiments on the formation of quantum superposition states in near-macroscopic systems raise the question of quantification of the sizes of general quantum superposition states (Leggett, 2002). The first method to quantify the cat-size measure was introduced by Leggett (1980): the so-called disconnectivity. However, a closer analysis of the disconnectivity shows that for indistinguishable particles this quantity is large even for no-superposition states, such as single-branch Fock states, due to the particle correlations induced by symmetrization.

In the last few years, several criteria have been developed to establish the effective size of macroscopic superpositions. Dur, Simon, and Cirac (2002) investigated a state having the form $|\phi_1\rangle^{\otimes M} + |\phi_2\rangle^{\otimes M}$, where the number of subsystems M is very large, but the states of the individual subsystems have large overlap equal to $1 - \epsilon^2$. They proposed two different methods for assigning an effective particle number to such states, using ideal Greenberger-Horne-Zeilinger states of the form $|0\rangle^{\otimes M} + |1\rangle^{\otimes M}$ as a standard of comparison. The two methods, based on decoherence and on a distillation protocol, lead to an effective size n of the order of $M\epsilon^2$. The adoption of this criterion to superconducting flux states provides a situation where counting the number of electrons that are involved in the two current-carrying states gives a large estimate for the size of the superposition, while a detailed analysis of how many electrons are actually behaving differently in the two branches gives a very different and much smaller value. The Dur, Simon, and Cirac criterion was later generalized by Marquardt, Abel, and von Delft (2008), who proposed a size measure based on counting how many single-particle operations are needed to map one state component (the "live cat") into the other one (the "dead cat").

A different approach was introduced by Korsbakken *et al.* (2007) who proposed a measure of size for such superposition states that are based on which measurements can be performed to probe and distinguish the different branches of the macroscopic superposition. This approach allows a comparison of the effective size for superposition states in very different physical systems. Comparison with the measure based on the analysis of coherence between branches (Leggett, 1980) indicates that this measurement-based measure provides significantly smaller effective superposition sizes. This criterion has been applied to macroscopic superposition states in flux qubits, revealing the effective size to be bounded by values in the range of 42–6000 (Korsbakken, Whaley, and Cirac, 2010).

While the Dur, Simon, and Cirac (2002) approach could not be applied to the present amplification scheme, the

Korsbakken *et al.* (2007) criterion for the effective size can be estimated by exploiting the previous results on the Bures distance between the macrostates. The problem of determining quantum states that can be deterministically discriminated can be directly related to the Bures distance between the involved states (Markham *et al.*, 2008). There it was shown that the probability of success of the discrimination p_{disc} between two states ρ_1 and ρ_2 fulfills the bound $p_{\mathrm{disc}}(\rho_1, \rho_2) \leq \mathcal{D}(\rho_1, \rho_2)$. According to Fig. 11, the Bures distance $\mathcal{D}(\mathcal{E}(|\Phi^+_{\mathrm{PC}}\rangle), \mathcal{E}(|\Phi^-_{\mathrm{PC}}\rangle))$ between two states decreases from 1 to 0.8 as soon as an average of one photon is lost. Accordingly, the close to perfect discrimination between the states $|\Phi^+_{\mathrm{PC}}\rangle$ and $|\Phi^-_{\mathrm{PC}}\rangle$ requires one to detect almost all particles. This result suggests that according to the Korsbakken *et al.*(2007) criterion the effective size of the macroscopic quantum superposition is rather limited, analogously to superconducting macrosuperposition. On the other hand, we note that the macrostates $|\Phi^{\phi}\rangle_B$ and $|\Phi^{\phi\perp}\rangle_B$ exhibit observables bearing macroscopically distinct average values even in the lossy regime with transmittivity T. Precisely, the average number of photons associated with the polarization mode $\vec{\pi}_\phi$ is $T\bar{m}$ for $|\Phi^{\phi\perp}\rangle_B$ and $T(3\bar{m}+1)$ for $|\Phi^{\phi}\rangle_B$. For the π mode $\vec{\pi}_{\phi\perp}$, orthogonal to $\vec{\pi}_\phi$, these values are interchanged between the two states. Hence we tend to agree with Korsbakken *et al.* (2007) that more general measurement strategy in order to compare the effective size of superposition states in different kinds of physical systems is at the present an open problem.

Other approaches have been proposed to quantify macroscopic quantum superposition. First, Bjork and Mana (2004) proposed an operational approach. Their size criterion for macroscopic superposition states is based on the fact that a superposition presents greater sensitivity in interferometric applications than its superposed constituent states. Lee and Jeong (2011) proposed to quantify the degree of quantum coherence and the effective size of the physical system that involves the superposition by exploiting quantum interference in phase space. Finally, Shimizu and Miyadera (2002, 2005) proposed an index of macroscopic entanglement based on correlation of local observables on many sites in macroscopic quantum systems.

VIII. WIGNER-FUNCTION THEORY

We now address the problem of providing a complete quantum phase-space analysis able to recognize the persistence of the QI-OPA properties in a decohering environment. Among the different representations of quantum states in the continuous-variable space (Cahill and Glauber, 1969), the Wigner quasiprobability representation has been widely exploited to investigate nonclassical properties, such as squeezing (Walls and Milburn, 1995) and EPR nonlocality (Banaszek and Wódkiewicz, 1998). In particular, the presence of negative quasiprobability regions has been considered as a consequence of the quantum superposition of distinct physical states (Bartlett, 1944). Note that, the negativity of the Wigner function is not the only parameter that allows one to estimate the nonclassicality of a certain state. For instance, the squeezed-vacuum state (Walls and Milburn, 1995) presents a positive W representation, while its properties

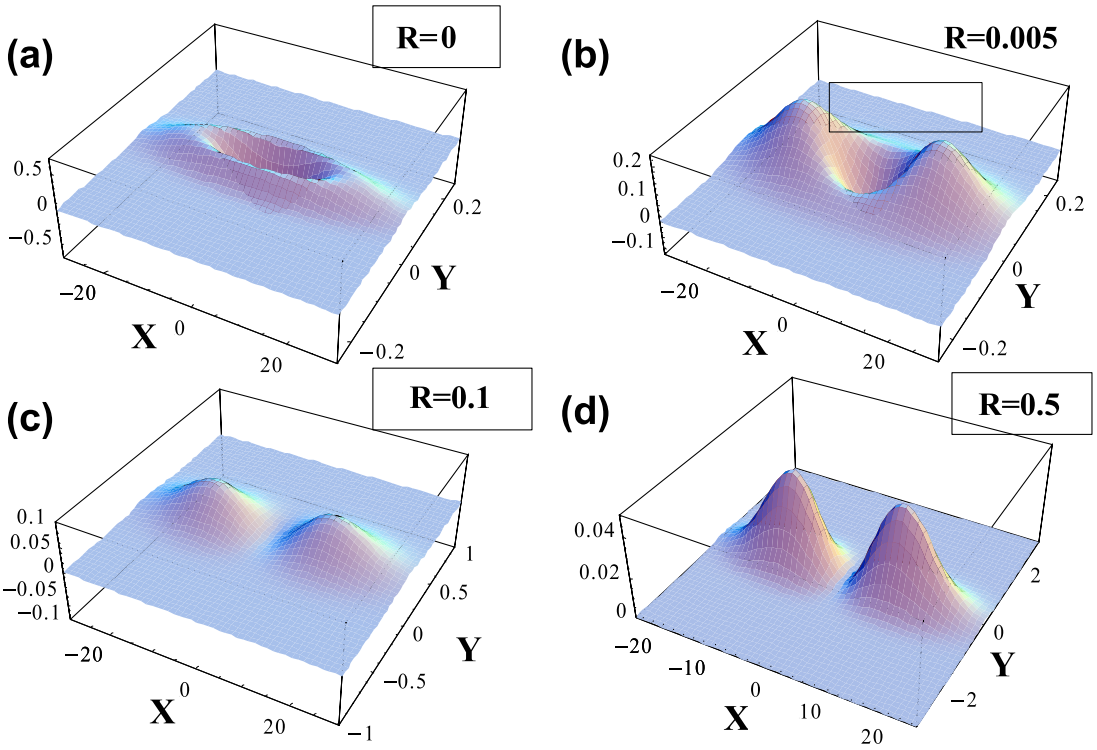

FIG. 12 (color online). Wigner function of a single-photon amplified state in a single-mode degenerate OPA for $g = 3$. (a) ($R = 0$.) Unperturbed case. (b) ($R = 0.005$.) For small reflectivity, the Wigner function remains negative in the central region. (c) ($R = 0.1$.) The Wigner function progressively evolves as a positive function in all the phase space. (d) ($R = 0.5$.) Transition from a nonpositive to a completely positive Wigner function. From Spagnolo *et al.*, 2009.

cannot be described by the laws of classical physics. Furthermore, recently it was shown that the Wigner function of an EPR state provides direct evidence of its nonlocal character (Cohen, 1997; Banaszek and Wódkiewicz, 1998), while being completely positive in all of the phase space.

In order to investigate the properties of the output field of the QI-OPA device in detail, we analyze the quasiprobability distribution introduced by Wigner, (1932) for the amplified field. The Wigner function is defined as the Fourier transform of the symmetrically ordered characteristic function $\chi(\eta)$ of the state described by the general density matrix $\hat{\rho}$,

$$\chi(\eta) = \mathrm{Tr}[\hat{\rho}\exp(\eta\hat{a}^\dagger - \eta^*\hat{a})]. \tag{23}$$

The associated Wigner function

$$W(\alpha) = \frac{1}{\pi^2}\int \exp(\eta^*\alpha - \eta\alpha^*)\chi(\eta)d^2\eta \tag{24}$$

exists for any $\hat{\rho}$ but is not always positive definite and, consequently, cannot be considered as a genuine probability distribution.

The properties of a multiphoton system have been investigated (Spagnolo *et al.*, 2009) in phase space by a Wigner quasiprobability function analysis when the fields propagate over a lossy channel. Figure 12(a) reports the ideal case, in the absence of losses, showing the presence of peculiar quantum properties such as squeezing and a nonpositive W representation. Then by investigating the resilience to losses of QI-OPA-amplified states in a lossy configuration, the persistence of the nonpositivity of the Wigner function was demonstrated in a certain range of the *system-environment* interaction parameter R. This behavior can be compared to the one shown by the $|\alpha\rangle$ states, MQS, which features a nonpositive W representation in the same interval of R. The more resilient structure of the QI-OPA-amplified states is shown by their slower decoherence rate, represented by both the slower decrease in the negative part of the Wigner function and by the behavior of the Bures distance between orthogonal macrostates (Spagnolo *et al.*, 2009). Since the negativity of the W representation is a sufficient but not a necessary condition for the nonclassicality of any physical system, future investigations should be aimed at the regime of decoherence in cases in which the Wigner function is completely positive, analyzing by different criteria the presence of the related quantum properties of the system.

IX. GENERATION OF MACRO-MACRO ENTANGLED STATES

One of the main challenges for an experimental test of entanglement in systems of large size is the realization of suitable criteria for the detection of entanglement in bipartite macroscopic systems. Great effort has been devoted in the last few years in this direction (Horodecki *et al.*, 2009). Some criteria, such as the partial transpose criterion developed by Horodecki, Horodecki, and Horodecki (1996) and Peres (1996), require the tomographic reconstruction of the density matrix, which from an experimental viewpoint is generally highly demanding for a system composed of a large number M of particles. However, the complete reconstruction of the state can be avoided by the entanglement witness method consisting of a class of tests where only a few significant local measurements are performed. For bipartite systems with large M, this approach was applied via collective measurements on the state. Within this context, Duan *et al.* proposed a general criterion based on measurements on continuous-variable observables (Duan *et al.*, 2000; Braunstein and van Loock, 2005). This general criterion was subsequently applied to the quantum extension of the Stokes parameters in order to obtain an entanglement bound for such variables (Korolkova *et al.*, 2002; Schnabel *et al.*, 2003; Korolkova and Loudon, 2005). Other approaches have been developed based on spin variables (Simon and Bouwmeester, 2003) or pseudo-Pauli operators (Chen *et al.*, 2002). An experimental application of this criterion based on collective spin measurements was performed in a bipartite system consisting of two separate gas samples (Julsgaard, Kozhekin, and Polzik, 2001).

The main experimental problem for such observations arises from the requirement of attaining a sufficient isolation of the quantum system from its environment, i.e., from the decoherence process (Zurek, 2003). An alternative approach to explain the quantum-to-classical transition was recently proposed by Kofler and Brukner, similar to an idea earlier discussed by Bell, Peres, and Mermin (Peres, 1993). They considered the emergence of classical physics in systems of increasing size within the domain of quantum theory (Kofler and Brukner, 2007). Precisely, they focused on the limits of the observability of quantum effects in macroscopic objects, showing that, for large systems, macrorealism arises under coarse-grained measurements. However, some counterexamples to such modelization were found later by Kofler and Brukner: some nonclassical Hamiltonians violate macrorealism in spite of coarse-grained measurements (Kofler and Brukner, 2008). Therefore the problem of the resolution within the measurement process appears to be a key ingredient in understanding the limits of the quantum behavior of macroscopic physical systems and the quantum-to-classical transition. Recently Jeong *et al.* contributed to the investigation of the possibility of observing the quantum features of a system under fuzzy measurement, by finding that extremely coarse-grained measurements can still be useful to reveal the quantum world where local realism fails (Jeong, Paternostro, and Ralph, 2009).

A. Macroscopic quantum state based on high-gain spontaneous parametric downconversion

We consider, once again, an optical parametric amplifier working in a high-gain regime: see Fig. 13. The radiation field under investigation is the quantum state obtained by SPDC (Kwiat *et al.*, 1995b; Eisenberg *et al.*, 2004), whose interaction Hamiltonian is $\mathcal{H}_U = \imath\hbar\chi(\hat{a}^\dagger_\pi\hat{b}^\dagger_{\pi_\perp} - \hat{a}^\dagger_{\pi_\perp}\hat{b}^\dagger_\pi) + \mathrm{H.c.}$

The output state reads (Simon and Bouwmeester, 2003; Eisenberg *et al.*, 2004; Caminati *et al.*, 2006b)

$$|\Psi^-\rangle = \frac{1}{C^2}\sum_{n=0}^{\infty}\Gamma^n\sqrt{n+1}||\psi_n^-\rangle \tag{25}$$

with

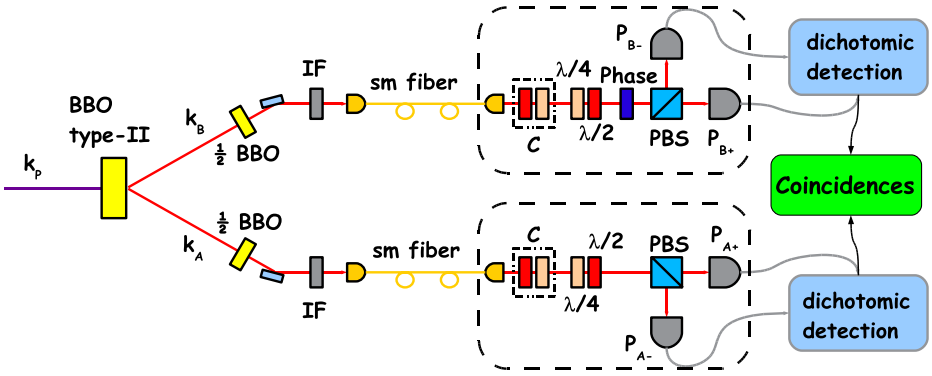

FIG. 13 (color online). Setup for the generation and detection of a bipartite macroscopic field. The high laser pulse in mode $\mathbf{k}_P$ excites a type-II noncollinear source in the high-gain regime ($g = 3.5$). The two spatial modes $\mathbf{k}_A$ and $\mathbf{k}_B$ are spectrally and spatially selected by interference filters (IFs) and single-mode fibers. After fiber compensation (C), the two modes are analyzed in polarization and detected by four photomultipliers. From Vitelli *et al.*, 2010b.

$$|\psi_n^-\rangle = \frac{1}{\sqrt{n+1}} \sum_{m=0}^{n} (-1)^m |(n-m)\pi, m\pi_\perp\rangle_A \times |m\pi, (n-m)\pi_\perp\rangle_B. \tag{26}$$

The output state can be written as the weighted coherent superposition of singlet spin-$n/2$ states $|\psi_n^-\rangle$.

This source has been adopted in many experiments, for different gain regimes. First, Kwiat *et al.* (1995b) exploited the polarization single state emitted in the single-pair regime to test the violation of Bell's inequalities (Genovese, 2005). Further work demonstrated experimentally four-photon entanglement in the second-order emission state of the SPDC source, by detecting the fourfold coincidences after the two output modes of the source were coupled to two 50:50 BS (Eibl *et al.*, 2003). Moreover, a generalized nonlocality test was also successfully performed with this configuration (Weinfurter and Zukowski, 2001). Later, a similar scheme was adopted by Wieczorek *et al.* (2008) to experimentally generate an entire family of four-photon entangled states.

1. Nonseparable Werner states

As mentioned, the presence of polarization entanglement in multiphoton states up to $M = 12$ photons was experimentally proved by investigating the high-loss regime in which at most one photon per branch was detected (Eisenberg *et al.*, 2004; Caminati *et al.*, 2006a). This approach consisted of the generation of a multiphoton state followed by a strong attenuation of both output branches of the SPDC scheme, in order to extract a correlated pair of photons, one for each branch (see Fig. 13). The method presents several advantages: First, the techniques for single-photon detection and characterization can be adopted. Second, it models the effect of loss associated with any communication process on a multiphoton entangled state.

The density matrix of the two-photon state was investigated by theory and experiment (Caminati *et al.*, 2006b). The state given by Eq. (25) is stochastically attenuated by a conventional beam-splitter model that simulates the propagation over a lossy channel. Then the density matrix of the two-photon state generated by postselection is expressed by

$$\rho_{\mathrm{SPDC}}^{\mathrm{HG}} = \begin{pmatrix} \frac{1-p}{4} & 0 & 0 & 0 \\ 0 & \frac{1+p}{4} & -\frac{p}{2} & 0 \\ 0 & -\frac{p}{2} & \frac{1+p}{4} & 0 \\ 0 & 0 & 0 & \frac{1-p}{4} \end{pmatrix} \tag{27}$$

with singlet weight $p = 1/(2\tilde{\Gamma}^2 + 1)$ and $\tilde{\Gamma} = (1-\eta)\tanh g$. Note that the density matrix $\rho_{\mathrm{SPDC}}^{\mathrm{HG}}$ is a Werner state, i.e., a weighted superposition of a maximally entangled singlet state and a fully mixed state (Werner, 1989). It is well known that the Werner states play a paradigmatic role in quantum information as they determine a family of mixed states including both entangled and separable states (Barbieri *et al.*, 2004). They model the decoherence process occurring in a singlet state traveling along a noisy channel, and hence they are adopted to investigate the distillation and concentration processes. Furthermore, depending on the singlet weight they can exhibit either entanglement and violation of Bell inequalities, or only entanglement, or separability. In the limit $\eta \to 0$ the above equation gives $\tilde{\Gamma} = \tanh g \approx 1$, for large g. With the hypothesis of very high losses, the singlet weight $p \geq \frac{1}{3}$ approaches the minimum value $\frac{1}{3}$. Since the condition $p > \frac{1}{3}$ implies the nonseparability condition for a general Werner state, the two-photon state is entangled for any large value of g. Figure 14 shows the result of the theory together with the experimental demonstration of bipartite entanglement for $M \leq 12$.

2. Quantum-to-classical transition by dichotomic measurement

We are now interested in analyzing the behavior of the system considered previously when the number of generated photons is increased and the system undergoes a fuzzy dichotomic measurement on the overall state, in which the generated particles cannot be addressed singularly. As shown by Chen *et al.* (2002), the demonstration of nonlocality in a multiphoton state produced by a nondegenerate optical parametric amplifier requires the experimental application of parity operators, with a detector efficiency $\eta = 1$. On the other hand, the estimation of a coarse-grained quantity through collective measurements as suggested by Portolan *et al.* (2006) misses the underlying quantum structure of the

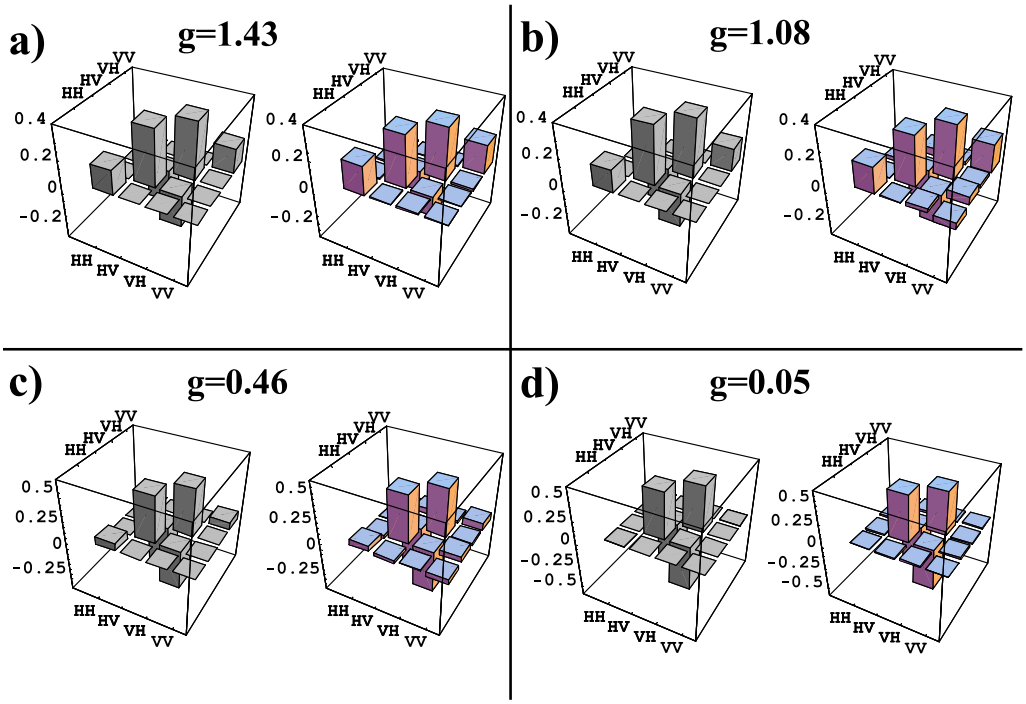

FIG. 14 (color online). Theoretical (left plots) and experimental (right plots) density matrices $\rho^{\mathrm{HG}}_{\mathrm{SPDC}}$ for different gain values. The experimental density matrices have been reconstructed by measuring 16 two-qubit observables. From Caminati *et al.*, 2006a.

generated state, introducing elements of local realism even in the presence of strong entanglement and in the absence of decoherence. A theoretical investigation on a multiphoton system generated by parametric downconversion was carried out by Reid, Munro, and De Martini (2002). They analyzed the possibility of testing the violation of Bell's inequality by performing a dichotomic measurement on the multiparticle quantum state. Precisely, in analogy with the spin formalism and the O-filter discrimination, they proposed to compare the number of photons polarized up with the number of photons polarized down at the exit of the amplifier: a dichotomic measurement on the multiphoton state. In such a way a small violation of the multiparticle Bell inequality can be revealed even in the presence of losses and of the quantum inefficiency of detectors. Once again, the violation decreases very rapidly for an increasing number M of the generated photons. Recently Bancal *et al.* (2008) discussed different techniques for testing the Bell inequality violation in multipair scenarios by performing a global measurement, in either Alice's or Bob's sites. According to their theory, the photon pairs were classified as distinguishable, i.e., independent, or indistinguishable, meaning that they belong to the same spatial and temporal mode. They found that while the state of indistinguishable pairs is more entangled, the state of independent pairs appears to be more nonlocal.

The possibility of observing quantum correlations in macroscopic systems through dichotomic measurement, by addressing two different measurement schemes, based on different dichotomization processes, was recently addressed by Vitelli *et al.* (2010b). More specifically, the persistence of nonlocality in a spin-$n/2$ singlet state with increasing size was investigated by studying the change in the correlation form as n increases, both in the ideal case and in the presence of losses. Two different types of dichotomic measurement on multiphoton states were considered: orthogonality filtering and threshold detection. Numerical simulation showed that interference-fringe patterns for singlet-$n/2$ states exhibit a transition from the sinusoidal pattern of the spin-$\frac{1}{2}$ state into a quasilinear pattern by increasing the number of photons associated with the spin state. According to this behavior a progressive decrease of the amount of violation is observed, as earlier predicted by Reid, Munro, and De Martini (2002)

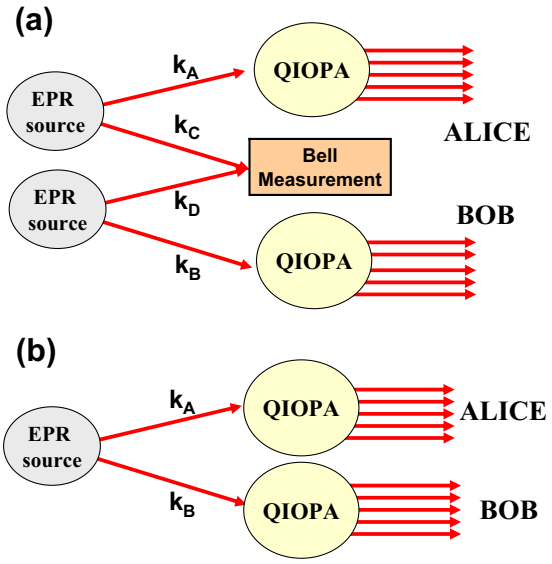

FIG. 15 (color online). Implementation of macro-macro entanglement (a) via entanglement swapping on two QI-OPAs and (b) through two optical parametric amplifiers. From De Martini, 2011.

and Bancal *et al.* (2008). All these results show that the dichotomic fuzzy measurements lack the necessary resolution to characterize such states. They also show, once again, how problematic is the experimental demonstration of quantum nonlocality of states with very large M.

B. Macroscopic quantum state by dual amplification of two-photon entangled state

The amplification schemes illustrated in Figs. 1(a)–1(c) could be upgraded in order to achieve an entangled macro-macro system showing nonlocality features (De Martini, 2011). Such a scheme could even exploit an entanglement swapping protocol as shown in Fig. 15(a) (Żukowski *et al.*, 1993; Pan *et al.*, 1998). There the final entangled state is achieved through a standard intermediate Bell measurement carried out on the single-photon states. A similar process has been suggested in several different contexts, e.g., to entangle micromechanical oscillators (Pirandola *et al.*, 2006). As an alternative approach, the single-photon states in modes k_A and k_B could be amplified by two independent QI-OPA's (see Fig. 15(b)). The resulting macro-macro scenario would be an interesting platform to perform loophole-free Bell inequalities.

It is an open question how to perform an entanglement and/or nonlocality test on the macro-macro states. Indeed, analogously to the micro-macro scenario, a coarse-grained measurement resolution would be needed. To overcome this challenge, it has been proposed to manipulate multiphoton quantum states obtained through optical parametric amplification by performing a measurement on a small portion of the output light field. Vitelli, Spagnolo, Sciarrino, and De Martini (2010) analyzed in detail the modifications of the quantum features of the macrostates by variation of the amount of extracted information and considered the best strategy to be adopted at the final measurement stage. Finally, it was found that the scheme does not allow one to violate any multiphoton Bell's inequality in the absence of auxiliary assumptions.

A similar investigation of the preprocessing of quantum macroscopic states of light generated by optimal quantum cloners in the presence of classical detection was carried out by Stobinska, Sekatski *et al.* (2011). They proposed a filter that selects two-mode high-number Fock states whose photon-number difference exceeds a certain value. This filter improves the distinguishability of some states by preserving the quantum macroscopic superposition (Stobinska, Toppel *et al.*, 2011). It is still an open question whether this filter can be efficiently implemented and whether it can lead to a genuine nonlocality test.

X. INTERACTION WITH A BOSE-EINSTEIN CONDENSATE

In recent years much interest has been attracted by the ambitious challenge of creating a macroscopic quantum superposition of a massive object by an entangled optomechanical interaction of a tiny mirror with a single photon trapped within a Michelson interferometer (Marshall *et al.*, 2003). This led to another realization of the well-known argument by Schrödinger (1935). A similar scheme could be considered which is based on the nonresonant scattering by a properly shaped *multiatom* Bose-Einstein condensate (BEC) of the

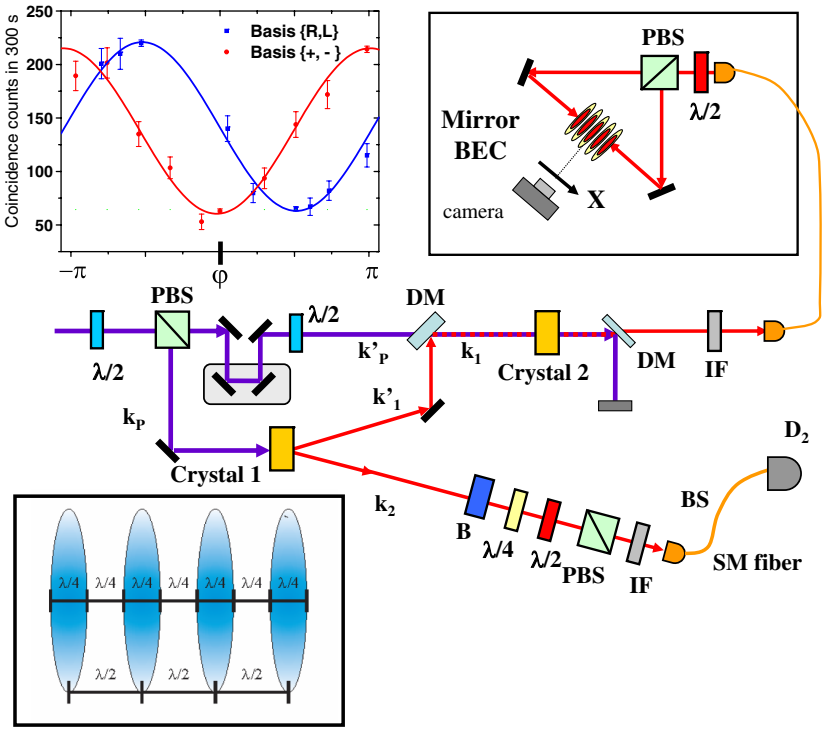

FIG. 16 (color online). Layout of the QI-OPA and mirror-BEC experimental apparatus. The upper left inset shows the interference patterns detected at the output of the PBS shown in the upper right inset for two different measurement bases $\{+, -\}$ and $\{L, R\}$. Alternating slabs of condensate and vacuum are shown in the lower left inset. From De Martini *et al.*, 2010.

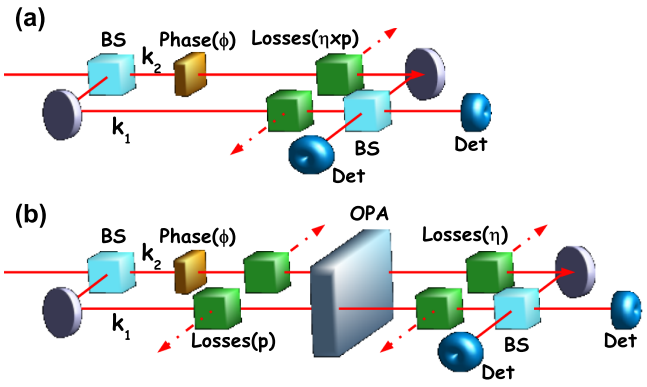

FIG. 17 (color online). Scheme for phase measurement. (a) Interferometric scheme adopted to estimate the phase (ϕ) introduced in the mode $\mathbf{k}_2$. (b) Interferometric scheme using a single photon and the optical parametric amplifier: the amplification of the single-photon state is performed before dominant losses. From Vitelli *et al.*, 2010a.

multiphoton state $|\Phi\rangle$ generated by a high-gain QI-OPA as described in Sec. II. Light scattering from BEC structures has been adopted so far to enhance their nonlinear macroscopic properties in superradiance experiments (Inouye, 1999), to show the possibility of matter-wave amplification (Kozume *et al.*, 1999), and nonlinear wave mixing (Deng *et al.*, 1999). The new scheme, represented by Fig. 16, results in a joint atom-photon micro-macro state entangled by momentum conservation. The resulting physical effect consists of the mechanical motion of a high-reflectivity optical multilayered Bragg-shaped mirror, referred to as a "mirror BEC," driven by the exchange of linear momentum with a photonic macrostate $|\Phi\rangle$.

The layout in Fig. 16 shows a QI-OPA system identical to the one represented in Fig. 1(c). The interfering polarization macrostates belonging to the quantum superposition (MQS) $|\Phi\rangle = 2^{-1/2}(|\Phi^{\phi}\rangle + |\Phi^{\phi\perp}\rangle)$ generated over mode k_2 are selected by a polarizing beam splitter and drive the mechanical motion of the mirror BEC along the X axis. Precisely, the displacements along the two opposite directions parallel to the X axis are driven, respectively, by the orthogonal polarizations $|\Phi^{\phi}\rangle$ and $|\Phi^{\phi\perp}\rangle$. Since these states are found to be entangled with the distant single photon emitted over the mode k_2, the same entanglement property can be transferred to the position macrostate of the optically driven mirror BEC. The discussion in Sec. V dealing with the entanglement processes can be extended to the present more complex optomechanical configuration.

XI. APPLICATIONS: FROM SENSING TO RADIOMETRY

A. Quantum sensing

The aim of quantum sensing is to develop strategies able to extract from a system the maximum amount of information with minimal disturbance. The possibility of performing precision measurements by adopting quantum resources can increase the achievable precision beyond the semiclassical regime of operation (Helstrom, 1976; Giovannetti, Lloyd, and Maccone, 2004, 2006). In the case of interferometry, this can be achieved by the use of the so-called $N00N$ states or squeezed states (Dur, 2002; Dur and Burnett, 2004), which are quantum-mechanical superpositions of just two terms, corresponding to all the available photons N being in either the signal arm or the reference arm of the interferometer. The use of $N00N$ states can enhance the precision in phase estimation to $1/N$, thus improving the scaling of the achievable precision with respect to the employed resources (Boto *et al.*, 2000; Dowling, 2008). This approach can have wide applications for minimally invasive sensing methods acting on quantum states. Nevertheless, these states are extremely fragile under unavoidable losses and decoherence (Gilbert and Weinstein, 2008). For instance, a sample whose phase shift is to be measured generally introduces attenuation. Since the quantum-enhanced modes of operations are generally very fragile, the impact of environmental effects can be much more harmful than in semiclassical schemes, completely destroying the quantum benefits (Rubin and Kaushik, 2007; Shaji and Caves, 2007). This scenario explains why overcoming the negative effects of realistic environments is the main challenge of the technology of quantum sensing. Recently the theoretical and experimental engineering of quantum states of light has attracted much attention, leading to the best possible precision in optical two-mode interferometry, even in the presence of experimental imperfections (Huver, Wildfeuer, and Dowling, 2008; Demkowicz-Dobrzanski *et al.*, 2009; Dorner *et al.*, 2009; Kacprowicz *et al.*, 2010; Lee, Jeong, and Jaksch, 2009; Maccone and De Cillis, 2009).

Recently Vitelli *et al.* (2010a) reported a hybrid approach based on a high-gain optical parametric amplifier operating for any polarization state in order to transfer quantum properties of different microscopic quantum states in the macroscopic regime: see Fig. 17. By performing the amplification of the microscopic probe after the interaction with the sample, it is possible to overcome the detrimental effects of losses on the phase measurement on the single-photon state following the test on the sample. This approach may be adopted in a minimally invasive scenario where a fragile sample, such as a biological system, requires a minimum amount of test photons in order to prevent damages. The action of the amplifier, i.e., the process of optimal phase-covariant quantum cloning, is to amplify the phase information which is codified in a single photon into a large number of particles. Such multiphoton states exhibit a high resilience to losses, as shown by De Martini, Sciarrino, and Vitelli (2008, 2009a, 2009b), and can be manipulated by exploiting a detection scheme which combines features of discrete and continuous variables. The effect of losses on the macroscopic field consists in the reduction of the detected signal and not in the complete cancellation of the phase information as in the single-photon probe case, thus improving the achievable sensitivity. This improvement consists of a constant enhancement $K(g)$ of the sensitivity, depending on the amplifier gain g. Hence, the sensitivity scales as $\sqrt{N}$, where N is the number of photons testing the sample, but the effect of the amplification process reduces the detrimental effect of losses by a factor proportional to the number of generated photons. Within this framework recently Escher, de Matos Filho, and Davidovich (2011) derived the general bounds on the adoption of quantum metrology in the presence of decoherence.

B. Quantum radiometry

Radiometry is the science of measuring the electromagnetic radiation. The available technologies in this field operate either in the relatively high-power regime or in the photon-counting regime based on the correlations of quantum fields. Recently a sophisticated radiometer apparatus was devised that works over a broad range of powers: from the single-photon level up to several tens of nanowatts, i.e., from the quantum to the classical regime (Sanguinetti *et al.*, 2010). In fact, such a system exploits the process of optimal quantum cloning and is able to provide an absolute measure of spectral radiance by relying on a particular aspect of the quantum-to-classical transition: as the number of information carriers (photons) grows, so does the cloning fidelity. Sanguinetti *et al.* showed that the fidelity of cloning can be used to produce an absolute power measurement with an uncertainty limited only by the uncertainty of a relative power measurement. They provided a convincing demonstration of this scheme by an all-fiber experiment at telecommunication wavelengths, by achieving an accuracy of 4%, a figure that can be easily improved by a dedicated metrology laboratory (Fasel *et al.*, 2002).

XII. CONCLUSIONS AND PERSPECTIVES

In this paper we reviewed several protocols and related experiments centered on the process of nonlinear amplification of single-photon quantum states. A large part of the investigation focused on a new protocol of quantum information, viz., the quantum-injected version of the OPA, by which a single photon, encoded as a microqubit, triggers'' by a QED process the generation of an in-principle unlimited number M of photons, i.e., a macroqubit, carrying a large portion of the information associated with the trigger particle. The seminal character of this protocol opened the way to the discovery, the realization, and the development of novel scientific methods and applications of fundamental and technical relevance. The quantum information protocols today generally referred to as quantum cloning, the quantum U-NOT gate, MQS, micro-macro entanglement, quantum reversion, or the quantum-to-classical transition were among the paradigmatic outcomes of the overall endeavor reported in this article, lasting more than one decade. In particular, the QI-OPA method was instrumental in the first experimental realization of the quantum-cloning process in several multiparticle regimes. This process was further thoroughly investigated, leading to the discovery of the U-NOT theorem and of the quantum reversion protocol and to the first experimental test of the no-signaling theorem. In this connection, the unexpected result of the experiment was that the impossibility of faster-than-light communication, i.e., the ''peaceful coexistence'' (according to Shimony) between special relativity and quantum mechanics, rests on the high-order correlations affecting the particles generated by a cloning machine.

A large part of the investigation focused on the realization via quantum cloning of the MQS process, which is related to the quantum-to-classical transition paradigm implied by the celebrated Schrödinger's cat argument (Schrödinger, 1935). Realization of the MQS process consisting of a large number of particles $M \geq 10^4$ was experimentally demonstrated, in a *nonentangled* configuration, by detection of the sinusoidal phase dependence of the interference-fringe patterns generated at the output of the apparatus. However, the bipartite micro-macro entanglement could be demonstrated only for a reduced number of particles, $M \leq 12$, owing to the existence of a detection loophole whose detrimental effect increases with M. A most interesting feature of the adopted MQS scheme was found to consist of its resilience to any externally driven decoherence process: this allowed the entire research to be carried out at $T = 300$ K. Accordingly, emphasis was given to extended theoretical analysis aimed at the understanding of this phase-impairing process affecting all multiparticle systems. The extension of the quantum-cloning argument to a novel macro-macro regime and the mechanical coherent interaction of a multiphoton MQS system with a multiatom BEC condensate were considered as proposals toward further research into the foundations of quantum mechanics.

Concerning the investigation of the quantum-to-classical transition, a set of entanglement criteria for bipartite systems of a large number of particles were introduced and analyzed in detail. In particular, a specific joint microscopic and macroscopic system based on optical parametric amplification of an entangled photon pair was addressed. The potential applications of these criteria of fundamental and technical relevance in different contexts were analyzed, e.g., the realization of nonlocality tests, quantum metrology, quantum sensing, and, as an open challenge for future research, the process of ''preselection, i.e., the establishment of efficient strategies able to generate and manipulate multiphoton states by performing measurements on a small portion of the output field (Vitelli, Spagnolo, Sciarrino, and De Martini, 2010). Precisely, within the macro-macro nonlocality test, the aim was to understand how the features of the macroqubit in the high-loss and large-photon-number regime are modified by varying the amount of extracted information and then to devise the best strategy to be adopted at the final measurement stage. In fact, the proposed preselection method, the simplest one based on the dichotomic measurement of the reflected part of the wave function in two different bases, did not allow violation of Bell's inequality. Finally, a more general approach to the micro-macro entanglement problem, based on single-photon–continuous- variable hybrid methods, was introduced (Spagnolo *et al.*, 2011). All these novel criteria and methods were considered and compared in the context of the existing literature in the field.

In summary, we believe that the extended theoretical and experimental investigation outlined by this Colloquium can contribute to open new paths of research either by stimulating the discovery of efficient theorems and protocols of quantum information processing, or, on the more fundamental side, by shedding additional light on the still uncertain border existing between the ''classical'' and the ''quantum'' aspects of nature.

ACKNOWLEDGMENTS

This work was supported by FIRB-Futuro in Ricerca (HYTEQ).

REFERENCES

Bae, J., and A. Acín, 2006, Phys. Rev. Lett. **97**, 030402.
Banaszek, K., and K. Wódkiewicz, 1998, Phys. Rev. A **58**, 4345.
Bancal, J. D., C. Branciard, N. Brunner, N. Gisin, S. Popescu, and C. Simon, 2008, Phys. Rev. A **78**, 062110.
Barbieri, M., F. De Martini, G. Di Nepi, and P. Mataloni, 2004, Phys. Rev. Lett. **92**, 177901.
Bartlett, M. S., 1944, Proc. Cambridge Philos. Soc. **41**, 71.
Bechmann-Pasquinucci, H., and N. Gisin, 1999, Phys. Rev. A **59**, 4238.
Bell, J. S., 1987, *Speakable and Unspeakable in Quantum Mechanics* (Cambridge University Press, Cambridge, England).
Bjork, G., and P. G. L. Mana, 2004, J. Opt. B **6**, 429.
Blinov, B., D. Moehring, L.-M. Duan, and C. Monroe, 2004, Nature (London) **428**, 153.
Boto, A. N., P. Kok, D. S. Abrams, S. L. Braunstein, C. P. Williams, and J. P. Dowling, 2000, Phys. Rev. Lett. **85**, 2733.
Bovino, F., F. De Martini, and V. Mussi, 1999, arXiv:quant-ph/9905048.
Boyd, R., 2008, *Nonlinear Optics* (Academic, New York).
Braunstein, S. L., and P. van Loock, 2005, Rev. Mod. Phys. **77**, 513.
Bruss, D., A. Ekert, and C. Macchiavello, 1998, Phys. Rev. Lett. **81**, 2598.
Bruß, D., M. Cinchetti, G. Mauro D'Ariano, and C. Macchiavello, 2000, Phys. Rev. A **62**, 012302.
Bruß, D., D. P. Di Vincenzo, A. Ekert, C. A. Fuchs, C. Macchiavello, and J. A. Smolin, 1998, Phys. Rev. A **57**, 2368.
Bures, D., 1969, Trans. Am. Math. Soc. **135**, 199.
Buzek, V., S. L. Braunstein, M. Hillery, and D. Bruß, 1997, Phys. Rev. A **56**, 3446.
Buzek, V., and M. Hillery, 1996, Phys. Rev. A **54**, 1844.
Buzek, V., and M. Hillery, 1998, Phys. Rev. Lett. **81**, 5003.
Buzek, V., M. Hillery, and R. F. Werner, 1999, Phys. Rev. A **60**, R2626.
Bužek, V., and M. Hillery, 2000, Phys. Rev. A **62**, 022303.
Cahill, K. E., and R. J. Glauber, 1969, Phys. Rev. **177**, 1882.
Caminati, M., F. De Martini, R. Perris, F. Sciarrino, and V. Secondi, 2006a, Phys. Rev. A **74**, 062304.
Caminati, M., F. De Martini, R. Perris, F. Sciarrino, and V. Secondi, 2006b, Phys. Rev. A **73**, 032312.
Caminati, M., F. De Martini, and F. Sciarrino, 2006, Laser Phys. **16**, 1551.
Cerf, N., and J. Fiurasek, 2006, Prog. Opt. **49**, 455.
Chen, Z.-B., J.-W. Pan, G. Hou, and Y.-D. Zhang, 2002, Phys. Rev. Lett. **88**, 040406.
Cohen, O., 1997, Phys. Rev. A **56**, 3484.
D'Ariano, G. M., and C. Macchiavello, 2003, Phys. Rev. A **67**, 042306.
De Angelis, T., E. Nagali, F. Sciarrino, and F. De Martini, 2007, Phys. Rev. Lett. **99**, 193601.
De Martini, F., 1998a, Phys. Rev. Lett. **81**, 2842.
De Martini, F., 1998b, Phys. Lett. A **250**, 15.
De Martini, F., 2011, Found. Phys. **41**, 363.
De Martini, F., V. Buzek, F. Sciarrino, and C. Sias, 2002, Nature (London) **419**, 815.
De Martini, F., V. Mussi, and F. Bovino, 2000, Opt. Commun. **179**, 581.
De Martini, F., D. Pelliccia, and F. Sciarrino, 2004, Phys. Rev. Lett. **92**, 067901.
De Martini, F., and F. Sciarrino, 2005, Prog. Quantum Electron. **29**, 165.
De Martini, F., F. Sciarrino, and V. Secondi, 2005, Phys. Rev. Lett. **95**, 240401.
De Martini, F., F. Sciarrino, and N. Spagnolo, 2009a, Phys. Rev. Lett. **103**, 100501.
De Martini, F., F. Sciarrino, and N. Spagnolo, 2009b, Phys. Rev. A **79**, 052305.
De Martini, F., F. Sciarrino, and C. Vitelli, 2008, Phys. Rev. Lett. **100**, 253601.
De Martini, F., F. Sciarrino, C. Vitelli, and F. S. Cataliotti, 2010, Phys. Rev. Lett. **104**, 050403.
Demkowicz-Dobrzanski, R., 2005, Phys. Rev. A **71**, 062321.
Demkowicz-Dobrzanski, R., U. Dorner, B. Smith, J. Lundeen, W. Wasilewski, K. Banaszek, and I. Walmsley, 2009, Phys. Rev. A **80**, 013825.
Deng, L., E. W. Hagley, J. Wen, M. Trippenbach, Y. Band, P. S. Julienne, J. E. Simsarian, K. Helmerson, S. L. Rolston, and W. D. Phillips, 1999, Nature (London) **398**, 218.
Derka, R., V. Buzek, and A. K. Ekert, 1998, Phys. Rev. Lett. **80**, 1571.
Dieks, D., 1982, Phys. Lett. **92A**, 271.
Dorner, U., R. Demkowicz-Dobrzanski, B. J. Smith, J. S. Lundeen, W. Wasilewski, K. Banaszek, and I. A. Walmsley, 2009, Phys. Rev. Lett. **102**, 040403.
Dowling, J. P., 2008, Contemp. Phys. **49**, 125.
Duan, L.-M., G. Giedke, J. I. Cirac, and P. Zoller, 2000, Phys. Rev. Lett. **84**, 2722.
Dur, J. A., 2002, Phys. Rev. A **66**, 041601.
Dur, J. A., and K. Burnett, 2004, Phys. Rev. A **70**, 033601.
Dur, W., C. Simon, and J. I. Cirac, 2002, Phys. Rev. Lett. **89**, 210402.
Eberhard, P. H., 1993, Phys. Rev. A **47**, R747.
Eibl, M., S. Gaertner, M. Bourennane, C. Kurtsiefer, M. Zukowski, and H. Weinfurter, 2003, Phys. Rev. Lett. **90**, 200403.
Eisenberg, H. S., G. H. Khoury, G. A. Durkin, C. Simon, and D. Bouwmeester, 2004, Phys. Rev. Lett. **93**, 193901.
Escher, B. M., R. L. de Matos Filho, and L. Davidovich, 2011, Nature Phys. **7**, 406.
Fasel, S., N. Gisin, G. Ribordy, V. Scarani, and H. Zbinden, 2002, Phys. Rev. Lett. **89**, 107901.
Genovese, M., 2005, Phys. Rep. **413**, 319.
Ghirardi, G., 1981, Referee Report to Foundation of Physics.
Gilbert, G., and Y. S. Weinstein, 2008, J. Mod. Opt. **55**, 3283.
Giovannetti, V., S. Lloyd, and L. Maccone, 2004, Science **306**, 1330.
Giovannetti, V., S. Lloyd, and L. Maccone, 2006, Phys. Rev. Lett. **96**, 010401.
Gisin, N., and S. Massar, 1997, Phys. Rev. Lett. **79**, 2153.
Gisin, N., and S. Popescu, 1999, Phys. Rev. Lett. **83**, 432.
Gisin, N., G. Ribordy, W. Tittel, and H. Zbinden, 2002, Rev. Mod. Phys. **74**, 145.
Greenberger, D. M., 1986, Ed., *New Techniques and Ideas in Quantum Measurement Theory* (Academy of Sciences, New York).
Groblacher, S., K. Hammerer, M. R. Vanner, and M. Aspelmeyer, 2009, Nature (London) **460**, 724.
Haroche, S., 2003, Proc. R. Soc. A **361**, 1339.
Helstrom, C. W., 1976, *Quantum Detection and Estimation Theory* (Academic Press, New York).
Herbert, N., 1982, Found. Phys. **12**, 1171.
Hong, C. K., Z. Y. Ou, and L. Mandel, 1987, Phys. Rev. Lett. **59**, 2044.
Horodecki, M., P. Horodecki, and R. Horodecki, 1996, Phys. Lett. A **223**, 1.
Horodecki, R., P. Horodecki, M. Horodecki, and K. Horodecki, 2009, Rev. Mod. Phys. **81**, 865.
Hubner, M., 1992, Phys. Lett. A **163**, 239.

Huver, S., C. Wildfeuer, and J. Dowling, 2008, Phys. Rev. A **78**, 063828.

Inouye, S., 1999, Science **285**, 571.

Irvine, W. T. M., A. Lamas Linares, M. J. A. de Dood, and D. Bouwmeester, 2004, Phys. Rev. Lett. **92**, 047902.

Jeong, H., M. Paternostro, and T. C. Ralph, 2009, Phys. Rev. Lett. **102**, 060403.

Jozsa, R., 1994, J. Mod. Opt. **41**, 2315.

Julsgaard, B., A. Kozhekin, and E. S. Polzik, 2001, Nature (London) **413**, 400.

Kacprowicz, M., R. Demkowicz-Dobrzanski, W. Wasilewski, K. Banaszek, and I. Walmsley, 2010, Nat. Photonics **4**, 357.

Kofler, J., and C. Brukner, 2007, Phys. Rev. Lett. **99**, 180403.

Kofler, J., and C. Brukner, 2008, Phys. Rev. Lett. **101**, 090403.

Korolkova, N., and R. Loudon, 2005, Phys. Rev. A **71**, 032343.

Korolkova, N., G. Leuchs, R. Loudon, T. C. Ralph, and C. Silberhorn, 2002, Phys. Rev. A **65**, 052306.

Korsbakken, J. I., K. B. Whaley, and J. I. Cirac, 2010, Europhys. Lett. **89**, 30 003.

Korsbakken, J. I., K. B. Whaley, J. Dubois, and J. I. Cirac, 2007, Phys. Rev. A **75**, 042106.

Kozume, M., Y. Suzuki, Y. Torii, T. Sugiura, T. Kuga, E. W. Hagley, and L. Deng, 1999, Science **286**, 2309.

Kwiat, P. G., K. Mattle, H. Weinfurter, A. Zeilinger, A. V. Sergienko, and Y. Shih, 1995a, Phys. Rev. Lett. **75**, 4337.

Kwiat, P. G., K. Mattle, H. Weinfurter, A. Zeilinger, A. V. Sergienko, and Y. Shih, 1995b, Phys. Rev. Lett. **75**, 4337.

Lamas-Linares, A., C. Simon, J. Howell, and D. Bouwmeester, 2002, Science **296**, 712.

Lee, C.-W., and H. Jeong, 2011, Phys. Rev. Lett. **106**, 220401.

Lee, S.-W., H. Jeong, and D. Jaksch, 2009, Phys. Rev. A **80**, 022104.

Leggett, A., 1980, Prog. Theor. Phys. **69**, 80.

Leggett, A., 2002, J. Phys. Condens. Matter **14**, R415.

Leibfried, D., R. Blatt, C. Monroe, and D. Wineland, 2003, Rev. Mod. Phys. **75**, 281.

Leibfried, D., *et al.*, 2005, Nature (London) **438**, 639.

Lu, C.-Y., X.-Q. Zhou, O. Gühne, W.-B. Gao, J. Zhang, Z.-S. Yuan, A. Goebel, T. Yang, and J.-W. Pan, 2007, Nature Phys. **3**, 91.

Maccone, L., and G. De Cillis, 2009, Phys. Rev. A **79**, 023812.

Mandel, L., 1983, Nature (London) **304**, 188.

Markham, D., J. A. Miszczak, Z. Puchala, and K. Zyczkowski, 2008, Phys. Rev. A **77**, 042111.

Marquardt, F., B. Abel, and J. von Delft, 2008, Phys. Rev. A **78**, 012109.

Marrucci, L., E. Karimi, S. Slussarenko, B. Piccirillo, E. Santamato, E. Nagali, and F. Sciarrino, 2011, J. Opt. **13**, 064001.

Marshall, W., C. Simon, R. Penrose, and D. Bouwmeester, 2003, Phys. Rev. Lett. **91**, 130401.

Massar, S., and S. Popescu, 1995, Phys. Rev. Lett. **74**, 1259.

Maudlin, T., 2002, *Quantum Nonlocality and Relativity* (Blackwell, Oxford).

Milonni, P., and M. Hardies, 1982, Phys. Lett. **92A**, 321.

Mollow, B. R., and R. J. Glauber, 1967, Phys. Rev. **160**, 1076.

Nagali, E., T. De Angelis, F. Sciarrino, and F. De Martini, 2007, Phys. Rev. A **76**, 042126.

Nagali, E., D. Giovannini, L. Marrucci, S. Slussarenko, E. Santamato, and F. Sciarrino, 2010, Phys. Rev. Lett. **105**, 073602.

Nagali, E., L. Sansoni, F. Sciarrino, F. De Martini, L. Marrucci, B. Piccirillo, E. Karimi, and E. Santamato, 2009, Nature Photon. **3**, 720.

Nielsen, M. A., and I. L. Chuang, 2000, *Quantum Information and Quantum Computation* (Cambridge University Press, Cambridge, England).

Ou, Z. Y., and L. Mandel, 1988, Phys. Rev. Lett. **61**, 50.

Ourjoumtsev, A., 2006, Science **312**, 83.

Ourjoumtsev, A., 2007, Nature (London) **448**, 784.

Pan, J.-W., D. Bouwmeester, H. Weinfurter, and A. Zeilinger, 1998, Phys. Rev. Lett. **80**, 3891.

Pelliccia, D., V. Schettini, F. Sciarrino, C. Sias, and F. De Martini, 2003, Phys. Rev. A **68**, 042306.

Peres, A., 1993, *Quantum Theory: Concepts and Methods* (Kluwer, Dordrecht).

Peres, A., 1996, Phys. Rev. Lett. **77**, 1413.

Pirandola, S., D. Vitali, P. Tombesi, and S. Lloyd, 2006, Phys. Rev. Lett. **97**, 150403.

Pomarico, E., B. Sanguinetti, P. Sekatski, H. Zbinden, and N. Gisin, 2011, New J. Phys. **13**, 063031.

Portolan, S., O. Di Stefano, S. Savasta, F. Rossi, and R. Girlanda, 2006, Phys. Rev. A **73**, 020101(R).

Raeisi, S., P. Sekatski, and C. Simon, 2011, Phys. Rev. Lett. **107**, 250401.

Raeisi, S., W. Tittel, and C. Simon, 2012, Phys. Rev. Lett. **108**, 120404.

Raimond, J. M., M. Brune, and S. Haroche, 2001, Rev. Mod. Phys. **73**, 565.

Rarity, J. G., and P. R. Tapster, 1990, Phys. Rev. Lett. **64**, 2495.

Reid, M. D., W. J. Munro, and F. De Martini, 2002, Phys. Rev. A **66**, 033801.

Ricci, M., F. Sciarrino, N. J. Cerf, R. Filip, J. Fiurasek, and F. D. Martini, 2005, Phys. Rev. Lett. **95**, 090504.

Ricci, M., F. Sciarrino, C. Sias, and F. De Martini, 2004, Phys. Rev. Lett. **92**, 047901.

Rocheleau, T., T. Ndukum, C. Macklin, J. B. Hertzberg, A. A. Clerk, and K. C. Schwab, 2010, Nature (London) **463**, 72.

Rubin, M. A., and S. Kaushik, 2007, Phys. Rev. A **75**, 053805.

Sanguinetti, B., E. Pomarico, P. Sekatski, H. Zbinden, and N. Gisin, 2010, Phys. Rev. Lett. **105**, 080503.

Scarani, V., S. Iblisdir, N. Gisin, and A. Acín, 2005, Rev. Mod. Phys. **77**, 1225.

Schleich, W., M. Pernigo, and F. Le Kien, 1991, Phys. Rev. A **44**, 2172.

Schnabel, R., W. P. Bowen, N. Treps, T. C. Ralph, H.-A. Bachor, and P. K. Lam, 2003, Phys. Rev. A **67**, 012316.

Schrödinger, E., 1935, Naturwissenschaften **23**, 807.

Sciarrino, F., and F. De Martini, 2005, Phys. Rev. A **72**, 062313.

Sciarrino, F., and F. De Martini, 2007, Phys. Rev. A **76**, 012330.

Sciarrino, F., V. Secondi, and F. De Martini, 2006, Phys. Rev. A **73**, 040303.

Sciarrino, F., C. Sias, M. Ricci, and F. De Martini, 2004a, Phys. Lett. A **323**, 34.

Sciarrino, F., C. Sias, M. Ricci, and F. De Martini, 2004b, Phys. Rev. A **70**, 052305.

Sekatski, P., N. Brunner, C. Branciard, N. Gisin, and C. Simon, 2009, Phys. Rev. Lett. **103**, 113601.

Sekatski, P., B. Sanguinetti, E. Pomarico, N. Gisin, and C. Simon, 2010, Phys. Rev. A **82**, 053814.

Shaji, A., and C. M. Caves, 2007, Phys. Rev. A **76**, 032111.

Shih, Y. H., and C. O. Alley, 1988, Phys. Rev. Lett. **61**, 2921.

Shimizu, A., and T. Miyadera, 2002, Phys. Rev. Lett. **89**, 270403.

Shimizu, A., and T. Miyadera, 2005, Phys. Rev. Lett. **95**, 090401.

Simon, C., and D. Bouwmeester, 2003, Phys. Rev. Lett. **91**, 053601.

Simon, C., V. Bužek, and N. Gisin, 2001, Phys. Rev. Lett. **87**, 170405.

Simon, C., G. Weihs, and A. Zeilinger, 2000, Phys. Rev. Lett. **84**, 2993.

Spagnolo, N., F. Sciarrino, and F. De Martini, 2010, Phys. Rev. A **82**, 032325.

Spagnolo, N., C. Vitelli, T. De Angelis, F. Sciarrino, and F. De Martini, 2009, Phys. Rev. A **80**, 032318.
Spagnolo, N., C. Vitelli, M. Paternostro, F. De Martini, and F. Sciarrino, 2011, Phys. Rev. A **84**, 032102.
Spagnolo, N., C. Vitelli, F. Sciarrino, and F. De Martini, 2010, Phys. Rev. A **82**, 052101.
Stobinska, M., P. Sekatski, A. Buraczewski, N. Gisin, and G. Leuchs, 2011, Phys. Rev. A **84**, 034104.
Stobinska, M., F. Toppel, P. Sekatski, A. Buraczewski, M. Zukowski, M. V. Chekhova, G. Leuchs, and N. Gisin, 2011, arXiv:1108.4906.
Teufel, J. D., 2011, Nature (London) **475**, 359.
van Enk, S. J., 2005, Phys. Rev. Lett. **95**, 010502.
Vitelli, C., N. Spagnolo, F. Sciarrino, and F. De Martini, 2010, Phys. Rev. A **82**, 062319.
Vitelli, C., N. Spagnolo, L. Toffoli, F. Sciarrino, and F. De Martini, 2010a, Phys. Rev. Lett. **105**, 113602.
Vitelli, C., N. Spagnolo, L. Toffoli, F. Sciarrino, and F. De Martini, 2010b, Phys. Rev. A **81**, 032123.
Walls, D. F., and G. J. Milburn, 1995, *Quantum Optics* (Springer, New York).
Weinfurter, H., and M. Zukowski, 2001, Phys. Rev. A **64**, 010102(R).
Werner, R. F., 1989, Phys. Rev. A **40**, 4277.
Werner, R. F., 1998, Phys. Rev. A **58**, 1827.
Wieczorek, W., C. Schmid, N. Kiesel, R. Pohlner, O. Ghne, and H. Weinfurter, 2008, Phys. Rev. Lett. **101**, 010503.
Wigner, E., 1932, Phys. Rev. **40**, 749.
Wootters, W., and W. Zurek, 1982, Nature (London) **299**, 802.
Yariv, A., 1989, *Quantum Electronics* (Wiley, New York)
Zhang, S., J. F. Chen, C. Liu, M. M. T. Loy, G. K. L. Wong, and S. Du, 2011, Phys. Rev. Lett. **106**, 243602
Zhao, Z., Y.-A. Chen, A.-N. Zhang, T. Yang, H. J. Briege, and J.-W. Pan, 2004, Nature (London) **430**, 54
Żukowski, M., A. Zeilinger, M. A. Horne, and A. K. Ekert, 1993, Phys. Rev. Lett. **71**, 4287.
Zurek, W. H., 2003, Rev. Mod. Phys. **75**, 715.